

Martin A Green

List of Publications by Year in descending order

Source: <https://exaly.com/author-pdf/6635359/publications.pdf>

Version: 2024-02-01

651
papers

68,686
citations

813

118
h-index

834

245
g-index

669
all docs

669
docs citations

669
times ranked

41000
citing authors

#	ARTICLE	IF	CITATIONS
1	The emergence of perovskite solar cells. <i>Nature Photonics</i> , 2014, 8, 506-514.	31.4	5,727
2	Surface plasmon enhanced silicon solar cells. <i>Journal of Applied Physics</i> , 2007, 101, 093105.	2.5	1,624
3	Solar cell efficiency tables (Version 45). <i>Progress in Photovoltaics: Research and Applications</i> , 2015, 23, 1-9.	8.1	1,618
4	Solar cell efficiency tables (version 54). <i>Progress in Photovoltaics: Research and Applications</i> , 2019, 27, 565-575.	8.1	1,096
5	Optical properties of intrinsic silicon at 300 K. <i>Progress in Photovoltaics: Research and Applications</i> , 1995, 3, 189-192.	8.1	1,069
6	Solar cell efficiency tables (version 39). <i>Progress in Photovoltaics: Research and Applications</i> , 2012, 20, 12-20.	8.1	1,047
7	Self-consistent optical parameters of intrinsic silicon at 300K including temperature coefficients. <i>Solar Energy Materials and Solar Cells</i> , 2008, 92, 1305-1310.	6.2	1,031
8	Improving solar cell efficiencies by down-conversion of high-energy photons. <i>Journal of Applied Physics</i> , 2002, 92, 1668-1674.	2.5	890
9	19.8% efficient "honeycomb" textured multicrystalline and 24.4% monocrystalline silicon solar cells. <i>Applied Physics Letters</i> , 1998, 73, 1991-1993.	3.3	854
10	Solar cell efficiency tables (version 50). <i>Progress in Photovoltaics: Research and Applications</i> , 2017, 25, 668-676.	8.1	792
11	Light trapping properties of pyramidally textured surfaces. <i>Journal of Applied Physics</i> , 1987, 62, 243-249.	2.5	791
12	Solar cell efficiency tables (version 57). <i>Progress in Photovoltaics: Research and Applications</i> , 2021, 29, 3-15.	8.1	787
13	Improving solar cell efficiencies by up-conversion of sub-band-gap light. <i>Journal of Applied Physics</i> , 2002, 92, 4117-4122.	2.5	753
14	Solar cell efficiency tables (version 51). <i>Progress in Photovoltaics: Research and Applications</i> , 2018, 26, 3-12.	8.1	729
15	Solar cell efficiency tables (Version 55). <i>Progress in Photovoltaics: Research and Applications</i> , 2020, 28, 3-15.	8.1	694
16	Solar cell efficiency tables (version 37). <i>Progress in Photovoltaics: Research and Applications</i> , 2011, 19, 84-92.	8.1	684
17	Solar cell efficiency tables (version 41). <i>Progress in Photovoltaics: Research and Applications</i> , 2013, 21, 1-11.	8.1	680
18	Solar cell efficiency tables (Version 53). <i>Progress in Photovoltaics: Research and Applications</i> , 2019, 27, 3-12.	8.1	655

#	ARTICLE	IF	CITATIONS
19	Cu ₂ ZnSnS ₄ solar cells with over 10% power conversion efficiency enabled by heterojunction heat treatment. <i>Nature Energy</i> , 2018, 3, 764-772.	39.5	623
20	22.8% efficient silicon solar cell. <i>Applied Physics Letters</i> , 1989, 55, 1363-1365.	3.3	619
21	Intrinsic concentration, effective densities of states, and effective mass in silicon. <i>Journal of Applied Physics</i> , 1990, 67, 2944-2954.	2.5	604
22	Solar cell efficiency tables (version 52). <i>Progress in Photovoltaics: Research and Applications</i> , 2018, 26, 427-436.	8.1	592
23	Solar cell efficiency tables (version 47). <i>Progress in Photovoltaics: Research and Applications</i> , 2016, 24, 3-11.	8.1	591
24	The path to 25% silicon solar cell efficiency: History of silicon cell evolution. <i>Progress in Photovoltaics: Research and Applications</i> , 2009, 17, 183-189.	8.1	586
25	Solar cell efficiency tables (version 49). <i>Progress in Photovoltaics: Research and Applications</i> , 2017, 25, 3-13.	8.1	582
26	Solar cell efficiency tables (version 48). <i>Progress in Photovoltaics: Research and Applications</i> , 2016, 24, 905-913.	8.1	574
27	24.5% Efficiency silicon PERT cells on MCZ substrates and 24.7% efficiency PERL cells on FZ substrates. <i>Progress in Photovoltaics: Research and Applications</i> , 1999, 7, 471-474.	8.1	571
28	Third generation photovoltaics: Ultra-high conversion efficiency at low cost. <i>Progress in Photovoltaics: Research and Applications</i> , 2001, 9, 123-135.	8.1	556
29	Silicon nanostructures for third generation photovoltaic solar cells. <i>Thin Solid Films</i> , 2006, 511-512, 654-662.	1.8	542
30	Energy conversion approaches and materials for high-efficiency photovoltaics. <i>Nature Materials</i> , 2017, 16, 23-34.	27.5	498
31	Efficient silicon light-emitting diodes. <i>Nature</i> , 2001, 412, 805-808.	27.8	496
32	Luminescent layers for enhanced silicon solar cell performance: Up-conversion. <i>Solar Energy Materials and Solar Cells</i> , 2007, 91, 829-842.	6.2	496
33	Solar cell efficiency tables (version 44). <i>Progress in Photovoltaics: Research and Applications</i> , 2014, 22, 701-710.	8.1	476
34	Solar cell efficiency tables (version 43). <i>Progress in Photovoltaics: Research and Applications</i> , 2014, 22, 1-9.	8.1	472
35	Solar cell efficiency tables (version 46). <i>Progress in Photovoltaics: Research and Applications</i> , 2015, 23, 805-812.	8.1	471
36	Solar cell efficiency tables (version 56). <i>Progress in Photovoltaics: Research and Applications</i> , 2020, 28, 629-638.	8.1	461

#	ARTICLE	IF	CITATIONS
37	Solar cell fill factors: General graph and empirical expressions. Solid-State Electronics, 1981, 24, 788-789.	1.4	452
38	Harnessing plasmonics for solar cells. Nature Photonics, 2012, 6, 130-132.	31.4	435
39	Plasmonics for photovoltaic applications. Solar Energy Materials and Solar Cells, 2010, 94, 1481-1486.	6.2	426
40	Benefit of Grain Boundaries in Organic-Inorganic Halide Planar Perovskite Solar Cells. Journal of Physical Chemistry Letters, 2015, 6, 875-880.	4.6	422
41	Solar cell efficiency tables (Version 60). Progress in Photovoltaics: Research and Applications, 2022, 30, 687-701.	8.1	406
42	Silicon quantum dot nanostructures for tandem photovoltaic cells. Thin Solid Films, 2008, 516, 6748-6756.	1.8	395
43	Thin-film solar cells: review of materials, technologies and commercial status. Journal of Materials Science: Materials in Electronics, 2007, 18, 15-19.	2.2	392
44	Beneficial Effects of PbI_2 Incorporated in Organolead Halide Perovskite Solar Cells. Advanced Energy Materials, 2016, 6, 1502104.	19.5	387
45	Optimized antireflection coatings for high-efficiency silicon solar cells. IEEE Transactions on Electron Devices, 1991, 38, 1925-1934.	3.0	380
46	Solar cell efficiency tables (version 36). Progress in Photovoltaics: Research and Applications, 2010, 18, 346-352.	8.1	380
47	Hole Transport Layer Free Inorganic $CsPbI_2$ Perovskite Solar Cell by Dual Source Thermal Evaporation. Advanced Energy Materials, 2016, 6, 1502202.	19.5	373
48	Solar cell efficiency tables (Version 58). Progress in Photovoltaics: Research and Applications, 2021, 29, 657-667.	8.1	363
49	Critical Role of Grain Boundaries for Ion Migration in Formamidinium and Methylammonium Lead Halide Perovskite Solar Cells. Advanced Energy Materials, 2016, 6, 1600330.	19.5	360
50	Lambertian light trapping in textured solar cells and light-emitting diodes: analytical solutions. Progress in Photovoltaics: Research and Applications, 2002, 10, 235-241.	8.1	351
51	Third generation photovoltaics: solar cells for 2020 and beyond. Physica E: Low-Dimensional Systems and Nanostructures, 2002, 14, 65-70.	2.7	343
52	Hydrothermal deposition of antimony selenosulfide thin films enables solar cells with 10% efficiency. Nature Energy, 2020, 5, 587-595.	39.5	338
53	Solar cell efficiency tables (version 40). Progress in Photovoltaics: Research and Applications, 2012, 20, 606-614.	8.1	333
54	The Passivated Emitter and Rear Cell (PERC): From conception to mass production. Solar Energy Materials and Solar Cells, 2015, 143, 190-197.	6.2	330

#	ARTICLE	IF	CITATIONS
55	Acoustic-optical phonon up-conversion and hot-phonon bottleneck in lead-halide perovskites. <i>Nature Communications</i> , 2017, 8, 14120.	12.8	330
56	Radiative efficiency of state-of-the-art photovoltaic cells. <i>Progress in Photovoltaics: Research and Applications</i> , 2012, 20, 472-476.	8.1	323
57	Over 9% Efficient Kesterite $\text{Cu}_2\text{ZnSnS}_4$ Solar Cell Fabricated by Using Zn^{1+} Cd^{1+} S Buffer Layer. <i>Advanced Energy Materials</i> , 2016, 6, 1600046.	19.5	322
58	The current status and future prospects of kesterite solar cells: a brief review. <i>Progress in Photovoltaics: Research and Applications</i> , 2016, 24, 879-898.	8.1	316
59	Strontium-Doped Low-Temperature-Processed CsPbI_2Br Perovskite Solar Cells. <i>ACS Energy Letters</i> , 2017, 2, 2319-2325.	17.4	314
60	Gas chromatography-mass spectrometry analyses of encapsulated stable perovskite solar cells. <i>Science</i> , 2020, 368, .	12.6	306
61	Solar Energy Conversion Toward 1 Terawatt. <i>MRS Bulletin</i> , 2008, 33, 355-364.	3.5	305
62	Perovskite Solar Cells: The Birth of a New Era in Photovoltaics. <i>ACS Energy Letters</i> , 2017, 2, 822-830.	17.4	305
63	Accuracy of analytical expressions for solar cell fill factors. <i>Solar Cells</i> , 1982, 7, 337-340.	0.6	304
64	Terawatt-scale photovoltaics: Trajectories and challenges. <i>Science</i> , 2017, 356, 141-143.	12.6	303
65	Solar cell efficiency tables (version 42). <i>Progress in Photovoltaics: Research and Applications</i> , 2013, 21, 827-837.	8.1	302
66	Solar cell efficiency tables (version 33). <i>Progress in Photovoltaics: Research and Applications</i> , 2009, 17, 85-94.	8.1	301
67	Mixed 3D-2D Passivation Treatment for Mixed-Cation Lead Mixed-Halide Perovskite Solar Cells for Higher Efficiency and Better Stability. <i>Advanced Energy Materials</i> , 2018, 8, 1703392.	19.5	289
68	Silicon quantum dot/crystalline silicon solar cells. <i>Nanotechnology</i> , 2008, 19, 245201.	2.6	288
69	Optical Properties of Photovoltaic Organic-Inorganic Lead Halide Perovskites. <i>Journal of Physical Chemistry Letters</i> , 2015, 6, 4774-4785.	4.6	280
70	Commercial progress and challenges for photovoltaics. <i>Nature Energy</i> , 2016, 1, .	39.5	278
71	Solar cell efficiency tables (Version 38). <i>Progress in Photovoltaics: Research and Applications</i> , 2011, 19, 565-572.	8.1	277
72	Efficiency enhancement of solar cells by luminescent up-conversion of sunlight. <i>Solar Energy Materials and Solar Cells</i> , 2006, 90, 3327-3338.	6.2	271

#	ARTICLE	IF	CITATIONS
73	General temperature dependence of solar cell performance and implications for device modelling. Progress in Photovoltaics: Research and Applications, 2003, 11, 333-340.	8.1	267
74	Twenty-four percent efficient silicon solar cells with double layer antireflection coatings and reduced resistance loss. Applied Physics Letters, 1995, 66, 3636-3638.	3.3	265
75	24% efficient silicon solar cells. Applied Physics Letters, 1990, 57, 602-604.	3.3	264
76	Humidity-Induced Degradation via Grain Boundaries of $\text{HC}(\text{NH}_2)_2 \times 2 \times \text{PbI}_3$ Planar Perovskite Solar Cells. Advanced Functional Materials, 2018, 28, 1705363.	14.9	260
77	Temperature dependence of the radiative recombination coefficient of intrinsic crystalline silicon. Journal of Applied Physics, 2003, 94, 4930.	2.5	257
78	Silicon quantum dot superlattices: Modeling of energy bands, densities of states, and mobilities for silicon tandem solar cell applications. Journal of Applied Physics, 2006, 99, 114902.	2.5	254
79	Solar cell efficiency tables (version 59). Progress in Photovoltaics: Research and Applications, 2022, 30, 3-12.	8.1	253
80	Fabrication of $\text{Cu}_2\text{ZnSnS}_4$ solar cells with 5.1% efficiency via thermal decomposition and reaction using a non-toxic sol-gel route. Journal of Materials Chemistry A, 2014, 2, 500-509.	10.3	249
81	Beyond 11% Efficient Sulfide Kesterite $\text{Cu}_2\text{ZnCdSnS}_4$ Solar Cell: Effects of Cadmium Alloying. ACS Energy Letters, 2017, 2, 930-936.	17.4	249
82	High-Efficiency Rubidium-Incorporated Perovskite Solar Cells by Gas Quenching. ACS Energy Letters, 2017, 2, 438-444.	17.4	247
83	Enhanced emission from Si-based light-emitting diodes using surface plasmons. Applied Physics Letters, 2006, 88, 161102.	3.3	242
84	Solar cell efficiency tables (version 35). Progress in Photovoltaics: Research and Applications, 2010, 18, 144-150.	8.1	239
85	CsPbBr_2 Perovskite Solar Cell by Spray-Assisted Deposition. ACS Energy Letters, 2016, 1, 573-577.	17.4	230
86	Crystalline and thin-film silicon solar cells: state of the art and future potential. Solar Energy, 2003, 74, 181-192.	6.1	228
87	Methylammonium Lead Bromide Perovskite-Based Solar Cells by Vapor-Assisted Deposition. Journal of Physical Chemistry C, 2015, 119, 3545-3549.	3.1	223
88	Crystalline silicon on glass (CSG) thin-film solar cell modules. Solar Energy, 2004, 77, 857-863.	6.1	216
89	Recent developments in photovoltaics. Solar Energy, 2004, 76, 3-8.	6.1	210
90	Hot carrier solar cells: Principles, materials and design. Physica E: Low-Dimensional Systems and Nanostructures, 2010, 42, 2862-2866.	2.7	192

#	ARTICLE	IF	CITATIONS
91	24% efficient per silicon solar cell: Recent improvements in high efficiency silicon cell research. Solar Energy Materials and Solar Cells, 1996, 41-42, 87-99.	6.2	188
92	Exploring Inorganic Binary Alkaline Halide to Passivate Defects in Low-Temperature-Processed Planar-Structure Hybrid Perovskite Solar Cells. Advanced Energy Materials, 2018, 8, 1800138.	19.5	186
93	Silicon photovoltaic modules: a brief history of the first 50 years. Progress in Photovoltaics: Research and Applications, 2005, 13, 447-455.	8.1	185
94	Improved value for the silicon intrinsic carrier concentration from 275 to 375 K. Journal of Applied Physics, 1991, 70, 846-854.	2.5	181
95	Solar cell efficiency tables (Version 34). Progress in Photovoltaics: Research and Applications, 2009, 17, 320-326.	8.1	180
96	Solar cell efficiency tables (Version 31). Progress in Photovoltaics: Research and Applications, 2008, 16, 61-67.	8.1	173
97	Large area efficient interface layer free monolithic perovskite/homo-junction-silicon tandem solar cell with over 20% efficiency. Energy and Environmental Science, 2018, 11, 2432-2443.	30.8	172
98	Defect trapping states and charge carrier recombination in organic-inorganic halide perovskites. Journal of Materials Chemistry C, 2016, 4, 793-800.	5.5	171
99	Accelerated Lifetime Testing of Organic-Inorganic Perovskite Solar Cells Encapsulated by Polyisobutylene. ACS Applied Materials & Interfaces, 2017, 9, 25073-25081.	8.0	165
100	Detailed balance limit for the series constrained two terminal tandem solar cell. Physica E: Low-Dimensional Systems and Nanostructures, 2002, 14, 96-100.	2.7	159
101	Very efficient light emission from bulk crystalline silicon. Applied Physics Letters, 2003, 82, 2996-2998.	3.3	151
102	Characterization of 23-percent efficient silicon solar cells. IEEE Transactions on Electron Devices, 1990, 37, 331-336.	3.0	147
103	Progress in Laser-Crystallized Thin-Film Polycrystalline Silicon Solar Cells: Intermediate Layers, Light Trapping, and Metallization. IEEE Journal of Photovoltaics, 2014, 4, 33-39.	2.5	144
104	655 mV open-circuit voltage, 17.6% efficient silicon MIS solar cells. Applied Physics Letters, 1979, 34, 790-793.	3.3	143
105	Solar energy collection by antennas. Solar Energy, 2002, 73, 395-401.	6.1	141
106	Slowing of carrier cooling in hot carrier solar cells. Thin Solid Films, 2008, 516, 6948-6953.	1.8	141
107	20% efficiency silicon solar cells. Applied Physics Letters, 1986, 48, 215-217.	3.3	136
108	Selective energy contacts for hot carrier solar cells. Thin Solid Films, 2008, 516, 6968-6973.	1.8	133

#	ARTICLE	IF	CITATIONS
109	Defect Control for 12.5% Efficiency Cu ₂ ZnSnSe ₄ Kesterite Thin-Film Solar Cells by Engineering of Local Chemical Environment. <i>Advanced Materials</i> , 2020, 32, e2005268.	21.0	133
110	Enhancing the Cu ₂ ZnSnS ₄ solar cell efficiency by back contact modification: Inserting a thin TiB ₂ intermediate layer at Cu ₂ ZnSnS ₄ /Mo interface. <i>Applied Physics Letters</i> , 2014, 104, .	3.3	131
111	Overcoming the Challenges of Large-Area High-Efficiency Perovskite Solar Cells. <i>ACS Energy Letters</i> , 2017, 2, 1978-1984.	17.4	130
112	Photovoltaics: technology overview. <i>Energy Policy</i> , 2000, 28, 989-998.	8.8	128
113	Effective light trapping in polycrystalline silicon thin-film solar cells by means of rear localized surface plasmons. <i>Applied Physics Letters</i> , 2010, 96, .	3.3	128
114	Integrated Photorechargeable Energy Storage System: Next-Generation Power Source Driving the Future. <i>Advanced Energy Materials</i> , 2020, 10, 1903930.	19.5	128
115	The effect of dielectric spacer thickness on surface plasmon enhanced solar cells for front and rear side depositions. <i>Journal of Applied Physics</i> , 2011, 109, .	2.5	125
116	n-Type silicon quantum dots and p-type crystalline silicon heteroface solar cells. <i>Solar Energy Materials and Solar Cells</i> , 2009, 93, 684-690.	6.2	123
117	How Did Solar Cells Get So Cheap?. <i>Joule</i> , 2019, 3, 631-633.	24.0	123
118	Photovoltaic principles. <i>Physica E: Low-Dimensional Systems and Nanostructures</i> , 2002, 14, 11-17.	2.7	121
119	Structural, electrical and photovoltaic characterization of Si nanocrystals embedded SiC matrix and Si nanocrystals/c-Si heterojunction devices. <i>Solar Energy Materials and Solar Cells</i> , 2008, 92, 474-481.	6.2	120
120	High performance light trapping textures for monocrystalline silicon solar cells. <i>Solar Energy Materials and Solar Cells</i> , 2001, 65, 369-375.	6.2	119
121	Synthesis and characterization of boron-doped Si quantum dots for all-Si quantum dot tandem solar cells. <i>Solar Energy Materials and Solar Cells</i> , 2009, 93, 273-279.	6.2	118
122	Beyond 8% ultrathin kesterite Cu ₂ ZnSnS ₄ solar cells by interface reaction route controlling and self-organized nanopattern at the back contact. <i>NPG Asia Materials</i> , 2017, 9, e401-e401.	7.9	118
123	Si nanocrystal p-i-n diodes fabricated on quartz substrates for third generation solar cell applications. <i>Applied Physics Letters</i> , 2009, 95, .	3.3	117
124	Nanoscale Microstructure and Chemistry of Cu ₂ ZnSnS ₄ /CdS Interface in Kesterite Cu ₂ ZnSnS ₄ Solar Cells. <i>Advanced Energy Materials</i> , 2016, 6, 1600706.	19.5	113
125	Manufacturing cost and market potential analysis of demonstrated roll-to-roll perovskite photovoltaic cell processes. <i>Solar Energy Materials and Solar Cells</i> , 2018, 174, 314-324.	6.2	113
126	Optical analysis of perovskite/silicon tandem solar cells. <i>Journal of Materials Chemistry C</i> , 2016, 4, 5679-5689.	5.5	112

#	ARTICLE	IF	CITATIONS
127	Cd-Free Cu ₂ ZnSnS ₄ solar cell with an efficiency greater than 10% enabled by Al ₂ O ₃ passivation layers. Energy and Environmental Science, 2019, 12, 2751-2764.	30.8	112
128	Solar cell efficiency tables (version 30). Progress in Photovoltaics: Research and Applications, 2007, 15, 425-430.	8.1	109
129	Light Illumination Induced Photoluminescence Enhancement and Quenching in Lead Halide Perovskite. Solar Rrl, 2017, 1, 1600001.	5.8	109
130	Solar cell efficiency tables. Progress in Photovoltaics: Research and Applications, 1993, 1, 25-29.	8.1	108
131	Progress on hot carrier cells. Solar Energy Materials and Solar Cells, 2009, 93, 713-719.	6.2	108
132	Mobile Charge-Induced Fluorescence Intermittency in Methylammonium Lead Bromide Perovskite. Nano Letters, 2015, 15, 4644-4649.	9.1	108
133	Consolidation of thin-film photovoltaic technology: the coming decade of opportunity. Progress in Photovoltaics: Research and Applications, 2006, 14, 383-392.	8.1	107
134	Estimates of te and in prices from direct mining of known ores. Progress in Photovoltaics: Research and Applications, 2009, 17, 347-359.	8.1	106
135	Intrinsic carrier concentration and minority carrier mobility of silicon from 77 to 300 K. Journal of Applied Physics, 1993, 73, 1214-1225.	2.5	105
136	Solar cell efficiency tables (version 28). Progress in Photovoltaics: Research and Applications, 2006, 14, 455-461.	8.1	105
137	Surface recombination velocity measurements at the silicon-silicon dioxide interface by microwave-detected photoconductance decay. Journal of Applied Physics, 1994, 76, 363-370.	2.5	104
138	Unveiling the Relationship between the Perovskite Precursor Solution and the Resulting Device Performance. Journal of the American Chemical Society, 2020, 142, 6251-6260.	13.7	103
139	Polaronic exciton binding energy in iodide and bromide organic-inorganic lead halide perovskites. Applied Physics Letters, 2015, 107, .	3.3	102
140	Balancing electrical and optical losses for efficient 4-terminal Si-perovskite solar cells with solution processed percolation electrodes. Journal of Materials Chemistry A, 2018, 6, 3583-3592.	10.3	102
141	Silicon Quantum Dots in a Dielectric Matrix for All-Silicon Tandem Solar Cells. Advances in OptoElectronics, 2007, 2007, 1-11.	0.6	101
142	Boosting the efficiency of pure sulfide CZTS solar cells using the In/Cd-based hybrid buffers. Solar Energy Materials and Solar Cells, 2016, 144, 700-706.	6.2	101
143	The Effect of Stoichiometry on the Stability of Inorganic Cesium Lead Mixed-Halide Perovskites Solar Cells. Journal of Physical Chemistry C, 2017, 121, 19642-19649.	3.1	101
144	Fabrication of Efficient and Stable CsPbI ₃ Perovskite Solar Cells through Cation Exchange Process. Advanced Energy Materials, 2019, 9, 1901685.	19.5	101

#	ARTICLE	IF	CITATIONS
145	Mobile Ion Induced Slow Carrier Dynamics in Organic-Inorganic Perovskite CH ₃ NH ₃ PbBr ₃ . ACS Applied Materials & Interfaces, 2016, 8, 5351-5357.	8.0	100
146	Very high efficiency silicon solar cells-science and technology. IEEE Transactions on Electron Devices, 1999, 46, 1940-1947.	3.0	99
147	Silicon solar cells: evolution, high-efficiency design and efficiency enhancements. Semiconductor Science and Technology, 1993, 8, 1-12.	2.0	97
148	Room temperature optical properties of organic-inorganic lead halide perovskites. Solar Energy Materials and Solar Cells, 2015, 137, 253-257.	6.2	96
149	Supercharging Silicon Solar Cell Performance by Means of Multijunction Concept. IEEE Journal of Photovoltaics, 2015, 5, 968-976.	2.5	96
150	21.8% Efficient Monolithic Perovskite/Homo-Junction-Silicon Tandem Solar Cell on 16 cm ² . ACS Energy Letters, 2018, 3, 2299-2300.	17.4	96
151	Fourier transform infrared spectroscopy of annealed silicon-rich silicon nitride thin films. Journal of Applied Physics, 2008, 104, .	2.5	95
152	Solution-Processed, Silver-Doped NiO _x as Hole Transporting Layer for High-Efficiency Inverted Perovskite Solar Cells. ACS Applied Energy Materials, 2018, 1, 561-570.	5.1	95
153	Pushing to the Limit: Radiative Efficiencies of Recent Mainstream and Emerging Solar Cells. ACS Energy Letters, 2019, 4, 1639-1644.	17.4	93
154	Solar cell efficiency tables (version 29). Progress in Photovoltaics: Research and Applications, 2007, 15, 35-40.	8.1	92
155	Impurity photovoltaic effect: Fundamental energy conversion efficiency limits. Journal of Applied Physics, 2002, 92, 1329-1336.	2.5	90
156	Time-Asymmetric Photovoltaics. Nano Letters, 2012, 12, 5985-5988.	9.1	90
157	Thermal Behavior of Photovoltaic Devices. , 2017, , .		90
158	Photovoltaic technology and visions for the future. Progress in Energy, 2019, 1, 013001.	10.9	90
159	Kesterite Solar Cells: Insights into Current Strategies and Challenges. Advanced Science, 2021, 8, 2004313.	11.2	90
160	Solar cell efficiency tables (version 27). Progress in Photovoltaics: Research and Applications, 2006, 14, 45-51.	8.1	89
161	Effects of Si-rich oxide layer stoichiometry on the structural and optical properties of Si QD/SiO ₂ multilayer films. Nanotechnology, 2009, 20, 485703.	2.6	88
162	High-efficiency PERL and PERT silicon solar cells on FZ and MCZ substrates. Solar Energy Materials and Solar Cells, 2001, 65, 429-435.	6.2	87

#	ARTICLE	IF	CITATIONS
163	Roadmap on optical energy conversion. <i>Journal of Optics (United Kingdom)</i> , 2016, 18, 073004.	2.2	85
164	Acetic Acid Assisted Crystallization Strategy for High Efficiency and Long-Term Stable Perovskite Solar Cell. <i>Advanced Science</i> , 2020, 7, 1903368.	11.2	85
165	Structural characterization of annealed Si _{1-x} C _x /SiC multilayers targeting formation of Si nanocrystals in a SiC matrix. <i>Journal of Applied Physics</i> , 2008, 103, 083544.	2.5	84
166	Morphology and Carrier Extraction Study of Organic-Inorganic Metal Halide Perovskite by One- and Two-Photon Fluorescence Microscopy. <i>Journal of Physical Chemistry Letters</i> , 2014, 5, 3849-3853.	4.6	84
167	Low-temperature growth of polycrystalline Ge thin film on glass by in situ deposition and ex situ solid-phase crystallization for photovoltaic applications. <i>Applied Surface Science</i> , 2009, 255, 7028-7035.	6.1	83
168	Realistic Silver Optical Constants for Plasmonics. <i>Scientific Reports</i> , 2016, 6, 30605.	3.3	83
169	Progress and outlook for high-efficiency crystalline silicon solar cells. <i>Solar Energy Materials and Solar Cells</i> , 2001, 65, 9-16.	6.2	82
170	Forty three per cent composite split-spectrum concentrator solar cell efficiency. <i>Progress in Photovoltaics: Research and Applications</i> , 2010, 18, 42-47.	8.1	82
171	Light- and bias-induced structural variations in metal halide perovskites. <i>Nature Communications</i> , 2019, 10, 444.	12.8	81
172	Emerging inorganic compound thin film photovoltaic materials: Progress, challenges and strategies. <i>Materials Today</i> , 2020, 41, 120-142.	14.2	81
173	Novel parallel multijunction solar cell. <i>Applied Physics Letters</i> , 1994, 65, 2907-2909.	3.3	80
174	Nucleation and Growth Control of HC(NH ₂) ₂ PbI ₃ for Planar Perovskite Solar Cell. <i>Journal of Physical Chemistry C</i> , 2016, 120, 11262-11267.	3.1	80
175	Phosphorus-doped silicon quantum dots for all-silicon quantum dot tandem solar cells. <i>Solar Energy Materials and Solar Cells</i> , 2009, 93, 1524-1530.	6.2	79
176	Solar cell efficiency tables (version 22). <i>Progress in Photovoltaics: Research and Applications</i> , 2003, 11, 347-352.	8.1	78
177	Perovskite cells charge forward. <i>Nature Materials</i> , 2015, 14, 559-561.	27.5	78
178	Accurate determination of minority carrier and lattice scattering mobility in silicon from photoconductance decay. <i>Journal of Applied Physics</i> , 1992, 72, 4161-4171.	2.5	77
179	Four-Terminal Tandem Solar Cells Using CH ₃ NH ₃ PbBr ₃ by Spectrum Splitting. <i>Journal of Physical Chemistry Letters</i> , 2015, 6, 3931-3934.	4.6	77
180	Electric field induced reversible and irreversible photoluminescence responses in methylammonium lead iodide perovskite. <i>Journal of Materials Chemistry C</i> , 2016, 4, 9060-9068.	5.5	77

#	ARTICLE	IF	CITATIONS
181	An effective method of predicting perovskite solar cell lifetime—Case study on planar CH ₃ NH ₃ PbI ₃ and HC(NH ₂) ₂ PbI ₃ perovskite solar cells and hole transfer materials of spiro-OMeTAD and PTAA. Solar Energy Materials and Solar Cells, 2017, 162, 41-46.	6.2	77
182	Spatially resolved analysis and minimization of resistive losses in high-efficiency Si solar cells. Progress in Photovoltaics: Research and Applications, 1996, 4, 399-414.	8.1	76
183	Photoluminescence and electroluminescence imaging of perovskite solar cells. Progress in Photovoltaics: Research and Applications, 2015, 23, 1697-1705.	8.1	76
184	Limiting loss mechanisms in 23% efficient silicon solar cells. Journal of Applied Physics, 1995, 77, 3491-3504.	2.5	75
185	Evolution of Si (and SiC) nanocrystal precipitation in SiC matrix. Thin Solid Films, 2008, 516, 3824-3830.	1.8	75
186	Thermophotonics. Semiconductor Science and Technology, 2003, 18, S270-S278.	2.0	74
187	Solar cell efficiency tables (Version 32). Progress in Photovoltaics: Research and Applications, 2008, 16, 435-440.	8.1	74
188	MIS solar cell—General theory and new experimental results for silicon. Applied Physics Letters, 1976, 29, 610-612.	3.3	73
189	Potential for low dimensional structures in photovoltaics. Materials Science and Engineering B: Solid-State Materials for Advanced Technology, 2000, 74, 118-124.	3.5	73
190	Modelling of hot carrier solar cell absorbers. Solar Energy Materials and Solar Cells, 2010, 94, 1516-1521.	6.2	73
191	40% efficient sunlight to electricity conversion. Progress in Photovoltaics: Research and Applications, 2015, 23, 685-691.	8.1	73
192	19.1% efficient silicon solar cell. Applied Physics Letters, 1984, 44, 1163-1164.	3.3	72
193	Limiting efficiency for current-constrained two-terminal tandem cell stacks. Progress in Photovoltaics: Research and Applications, 2002, 10, 299-307.	8.1	72
194	Recent progress and future prospects of perovskite tandem solar cells. Applied Physics Reviews, 2021, 8, .	11.3	71
195	Effects of boron doping on the structural and optical properties of silicon nanocrystals in a silicon dioxide matrix. Nanotechnology, 2008, 19, 424019.	2.6	70
196	Spin-coating free fabrication for highly efficient perovskite solar cells. Solar Energy Materials and Solar Cells, 2017, 168, 165-171.	6.2	70
197	16.7% efficient, laser textured, buried contact polycrystalline silicon solar cell. Applied Physics Letters, 1989, 55, 2363-2365.	3.3	69
198	High-efficiency silicon solar cells: Full factor limitations and non-ideal diode behaviour due to voltage-dependent rear surface recombination velocity. Progress in Photovoltaics: Research and Applications, 1993, 1, 133-143.	8.1	69

#	ARTICLE	IF	CITATIONS
199	Temperature dependent optical properties of CH ₃ NH ₃ PbI ₃ perovskite by spectroscopic ellipsometry. Applied Physics Letters, 2016, 108, .	3.3	68
200	The Role of Hydrogen from ALD Al ₂ O ₃ in Kesterite Cu ₂ ZnSnS ₄ Solar Cells: Grain Surface Passivation. Advanced Energy Materials, 2018, 8, 1701940.	19.5	68
201	Multiple band and impurity photovoltaic solar cells: General theory and comparison to tandem cells. Progress in Photovoltaics: Research and Applications, 2001, 9, 137-144.	8.1	67
202	Polycrystalline silicon on glass for thin-film solar cells. Applied Physics A: Materials Science and Processing, 2009, 96, 153-159.	2.3	67
203	Investigation of theoretical efficiency limit of hot carriers solar cells with a bulk indium nitride absorber. Journal of Applied Physics, 2010, 108, .	2.5	67
204	Thin-film polycrystalline silicon solar cells formed by diode laser crystallisation. Progress in Photovoltaics: Research and Applications, 2013, 21, 1377-1383.	8.1	67
205	Dynamic study of the light soaking effect on perovskite solar cells by in-situ photoluminescence microscopy. Nano Energy, 2018, 46, 356-364.	16.0	67
206	24.5% efficiency PERT silicon solar cells on SEH MCZ substrates and cell performance on other SEH CZ and FZ substrates. Solar Energy Materials and Solar Cells, 2001, 66, 27-36.	6.2	66
207	Role of the interface for the electronic structure of Si quantum dots. Physical Review B, 2008, 78, .	3.2	66
208	Effects of phosphorus doping on structural and optical properties of silicon nanocrystals in a SiO ₂ matrix. Thin Solid Films, 2009, 517, 5646-5652.	1.8	66
209	Enhanced Heterojunction Interface Quality To Achieve 9.3% Efficient Cd-Free Cu ₂ ZnSnS ₄ Solar Cells Using Atomic Layer Deposition ZnSnO Buffer Layer. Chemistry of Materials, 2018, 30, 7860-7871.	6.7	66
210	Large area, concentrator buried contact solar cells. IEEE Transactions on Electron Devices, 1995, 42, 144-149.	3.0	64
211	Limiting efficiency of bulk and thin-film silicon solar cells in the presence of surface recombination. Progress in Photovoltaics: Research and Applications, 1999, 7, 327-330.	8.1	64
212	Enhanced light trapping for high efficiency crystalline solar cells by the application of rear surface plasmons. Solar Energy Materials and Solar Cells, 2012, 101, 217-226.	6.2	64
213	Silicon quantum dot based solar cells: addressing the issues of doping, voltage and current transport. Progress in Photovoltaics: Research and Applications, 2011, 19, 813-824.	8.1	63
214	Evidence for multiple barrier heights in P-type PtSi Schottky-barrier diodes from I-V-T and photoresponse measurements. Solid-State Electronics, 1990, 33, 299-308.	1.4	62
215	The impurity photovoltaic (IPV) effect in wide-bandgap semiconductors: an opportunity for very-high-efficiency solar cells?. Progress in Photovoltaics: Research and Applications, 2002, 10, 345-353.	8.1	62
216	Spatial Distribution of Lead Iodide and Local Passivation on Organo-Lead Halide Perovskite. ACS Applied Materials & Interfaces, 2017, 9, 6072-6078.	8.0	62

#	ARTICLE	IF	CITATIONS
217	Interplay between the hot phonon effect and intervalley scattering on the cooling rate of hot carriers in GaAs and InP. <i>Progress in Photovoltaics: Research and Applications</i> , 2012, 20, 82-92.	8.1	61
218	Characterization of high-efficiency silicon solar cells. <i>Journal of Applied Physics</i> , 1985, 58, 4402-4408.	2.5	60
219	Limiting efficiency for a multi-band solar cell containing three and four bands. <i>Physica E: Low-Dimensional Systems and Nanostructures</i> , 2002, 14, 121-125.	2.7	60
220	Formation and photoluminescence of Si quantum dots in SiO ₂ /Si ₃ N ₄ hybrid matrix for all-Si tandem solar cells. <i>Solar Energy Materials and Solar Cells</i> , 2010, 94, 2238-2243.	6.2	60
221	Large-Area Diode Laser Defect Annealing of Polycrystalline Silicon Solar Cells. <i>IEEE Transactions on Electron Devices</i> , 2012, 59, 2838-2841.	3.0	60
222	Silicon nanocrystals in an oxide matrix for thin film solar cells with 492mV open circuit voltage. <i>Solar Energy Materials and Solar Cells</i> , 2012, 100, 65-68.	6.2	60
223	Ag requirements for silicon wafer-based solar cells. <i>Progress in Photovoltaics: Research and Applications</i> , 2011, 19, 911-916.	8.1	58
224	Highly efficient copper-rich chalcopyrite solar cells from DMF molecular solution. <i>Nano Energy</i> , 2020, 69, 104438.	16.0	57
225	High Efficiency Cu ₂ ZnSn(S,Se) ₄ Solar Cells with Shallow Li _{Zn} Acceptor Defects Enabled by Solution-Based Li Post-Deposition Treatment. <i>Advanced Energy Materials</i> , 2021, 11, 2003783.	19.5	57
226	17.8-percent efficiency polycrystalline silicon solar cells. <i>IEEE Transactions on Electron Devices</i> , 1990, 37, 382-384.	3.0	56
227	High efficiency polycrystalline silicon solar cells using phosphorus pretreatment. <i>Applied Physics Letters</i> , 1986, 48, 873-875.	3.3	55
228	Improved value for the silicon intrinsic carrier concentration at 300 K. <i>Applied Physics Letters</i> , 1990, 57, 255-257.	3.3	55
229	A conceptual model of light coupling by pillar diffraction gratings. <i>Journal of Applied Physics</i> , 2007, 101, 063105.	2.5	55
230	Ultrafast Carrier Dynamics in Methylammonium Lead Bromide Perovskite. <i>Journal of Physical Chemistry C</i> , 2016, 120, 2542-2547.	3.1	54
231	Efficiency Enhancement of Kesterite Cu ₂ ZnSnS ₄ Solar Cells via Solution-Processed Ultrathin Tin Oxide Intermediate Layer at Absorber/Buffer Interface. <i>ACS Applied Energy Materials</i> , 2018, 1, 154-160.	5.1	53
232	Elucidating Mechanisms behind Ambient Storage-Induced Efficiency Improvements in Perovskite Solar Cells. <i>ACS Energy Letters</i> , 2021, 6, 925-933.	17.4	52
233	Solar Cell Efficiency Tables (Version 20). <i>Progress in Photovoltaics: Research and Applications</i> , 2002, 10, 355-360.	8.1	51
234	Enhanced evanescent mode light trapping in organic solar cells and other low index optoelectronic devices. <i>Progress in Photovoltaics: Research and Applications</i> , 2011, 19, 473-477.	8.1	51

#	ARTICLE	IF	CITATIONS
235	Solar cell efficiency tables (version 17). Progress in Photovoltaics: Research and Applications, 2001, 9, 49-56.	8.1	50
236	Fabrication and electrical characteristics of Si nanocrystal/c-Si heterojunctions. Applied Physics Letters, 2007, 91, 123510.	3.3	50
237	A full thermal model for photovoltaic devices. Solar Energy, 2016, 140, 73-82.	6.1	50
238	Lessons Learnt from Spatially Resolved Electrochemical and Photoluminescence Imaging: Interfacial Delamination in $\text{CH}_3\text{NH}_3\text{PbI}_3$ Planar Perovskite Solar Cells upon Illumination. Advanced Energy Materials, 2017, 7, 1602111.	19.5	50
239	Quasi-Vertically-Orientated Antimony Sulfide Inorganic Thin-Film Solar Cells Achieved by Vapor Transport Deposition. ACS Applied Materials & Interfaces, 2020, 12, 22825-22834.	8.0	50
240	Utilization of Direct and Diffuse Sunlight in a Dye-Sensitized Solar Cell $\text{p}^+\text{-Si}$ Silicon Photovoltaic Hybrid Concentrator System. Journal of Physical Chemistry Letters, 2011, 2, 581-585.	4.6	49
241	Non-ideal energy selective contacts and their effect on the performance of a hot carrier solar cell with an indium nitride absorber. Applied Physics Letters, 2012, 100, .	3.3	49
242	Flexible kesterite $\text{Cu}_2\text{ZnSnS}_4$ solar cells with sodium-doped molybdenum back contacts on stainless steel substrates. Solar Energy Materials and Solar Cells, 2018, 182, 14-20.	6.2	49
243	Generalized relationship between dark carrier distribution and photocarrier collection in solar cells. Journal of Applied Physics, 1997, 81, 268-271.	2.5	48
244	Intermediate band solar cell with many bands: Ideal performance. Journal of Applied Physics, 2003, 94, 6150-6158.	2.5	48
245	General solar cell curve factors including the effects of ideality factor, temperature and series resistance. Solid-State Electronics, 1977, 20, 265-266.	1.4	47
246	Effects of pinholes, oxide traps, and surface states on MIS solar cells. Applied Physics Letters, 1978, 33, 178-180.	3.3	47
247	Departures from the principle of superposition in silicon solar cells. Journal of Applied Physics, 1994, 76, 7920-7930.	2.5	47
248	Comment on "Three-dimensional photonic-crystal emitter for thermal photovoltaic power generation" [Appl. Phys. Lett. 83, 380 (2003)]. Applied Physics Letters, 2004, 84, 1997-1998.	3.3	47
249	Clear quantum-confined luminescence from crystalline silicon/ SiO_2 single quantum wells. Applied Physics Letters, 2004, 84, 2286-2288.	3.3	47
250	Spatially resolved photoluminescence imaging of essential silicon solar cell parameters and comparison with CELLO measurements. Solar Energy Materials and Solar Cells, 2013, 109, 77-81.	6.2	47
251	Two-dimensional numerical optimization study of the rear contact geometry of high-efficiency silicon solar cells. Journal of Applied Physics, 1994, 75, 5391-5405.	2.5	46
252	Fabrication and characterization of Si nanocrystals in SiC matrix produced by magnetron cosputtering. Journal of Vacuum Science & Technology B, 2007, 25, 1327-1335.	1.3	46

#	ARTICLE	IF	CITATIONS
253	Do built-in fields improve solar cell performance?. Progress in Photovoltaics: Research and Applications, 2009, 17, 57-66.	8.1	46
254	The Impact of a Dynamic Two-Step Solution Process on Film Formation of Cs _{0.15} (MA _{0.7} FA _{0.3}) _{0.85} PbI ₃ Perovskite and Solar Cell Performance. Small, 2019, 15, e1804858.	10.0	46
255	Beyond 10% efficiency Cu ₂ ZnSnS ₄ solar cells enabled by modifying the heterojunction interface chemistry. Journal of Materials Chemistry A, 2019, 7, 27289-27296.	10.3	46
256	Extended infrared response of silicon solar cells and the impurity photovoltaic effect. Solar Energy Materials and Solar Cells, 1996, 41-42, 195-204.	6.2	45
257	Numerical quantification and minimization of perimeter losses in high-efficiency silicon solar cells. Progress in Photovoltaics: Research and Applications, 1996, 4, 355-367.	8.1	45
258	Solar cell efficiency tables (version 15). Progress in Photovoltaics: Research and Applications, 2000, 8, 187-195.	8.1	45
259	Limiting photovoltaic monochromatic light conversion efficiency. Progress in Photovoltaics: Research and Applications, 2001, 9, 257-261.	8.1	45
260	Ultimate efficiency limit of single-junction perovskite and dual-junction perovskite/silicon two-terminal devices. Japanese Journal of Applied Physics, 2015, 54, 08KD04.	1.5	45
261	Improved estimates for Te and Se availability from Cu anode slimes and recent price trends. Progress in Photovoltaics: Research and Applications, 2006, 14, 743-751.	8.1	44
262	Solar cell efficiency tables (version 11). Progress in Photovoltaics: Research and Applications, 1998, 6, 35-42.	8.1	43
263	SHORT COMMUNICATION: Solar cell efficiency tables (version 25). Progress in Photovoltaics: Research and Applications, 2005, 13, 49-54.	8.1	43
264	Lifetime limiting recombination pathway in thin-film polycrystalline silicon on glass solar cells. Journal of Applied Physics, 2010, 107, 123705.	2.5	43
265	Formation of heavily boron-doped hydrogenated polycrystalline germanium thin films by co-sputtering for developing p+ emitters of bottom cells. Solar Energy Materials and Solar Cells, 2011, 95, 981-985.	6.2	43
266	Rapid thermal annealing and crystallization mechanisms study of silicon nanocrystal in silicon carbide matrix. Nanoscale Research Letters, 2011, 6, 129.	5.7	42
267	Formation and photoluminescence of Si nanocrystals in controlled multilayer structure comprising of Si-rich nitride and ultrathin silicon nitride barrier layers. Thin Solid Films, 2011, 519, 5408-5412.	1.8	42
268	Silicon solar cells: state of the art. Philosophical Transactions Series A, Mathematical, Physical, and Engineering Sciences, 2013, 371, 20110413.	3.4	42
269	Recombination rate saturation mechanisms at oxidized surfaces of high-efficiency silicon solar cells. Journal of Applied Physics, 1995, 78, 4740-4754.	2.5	41
270	Excitons in silicon diodes and solar cells: A three-particle theory. Journal of Applied Physics, 1996, 79, 195-203.	2.5	41

#	ARTICLE	IF	CITATIONS
271	Prospects for photovoltaic efficiency enhancement using low-dimensional structures. <i>Nanotechnology</i> , 2000, 11, 401-405.	2.6	41
272	Solar cell efficiency tables (version 18). <i>Progress in Photovoltaics: Research and Applications</i> , 2001, 9, 287-293.	8.1	41
273	Blue-violet photoluminescence from colloidal suspension of nanocrystalline silicon in silicon oxide matrix. <i>Solid State Communications</i> , 2009, 149, 352-356.	1.9	41
274	Epitaxial Cu ₂ ZnSnS ₄ thin film on Si (111) 4° substrate. <i>Applied Physics Letters</i> , 2015, 106, .	3.3	41
275	Transparent Electrodes Consisting of a Surface-Treated Buffer Layer Based on Tungsten Oxide for Semitransparent Perovskite Solar Cells and Four-Terminal Tandem Applications. <i>Small Methods</i> , 2020, 4, 2000074.	8.6	41
276	A 15% efficient silicon MIS solar cell. <i>Applied Physics Letters</i> , 1978, 33, 637-639.	3.3	40
277	Monolithic Wide Band Gap Perovskite/Perovskite Tandem Solar Cells with Organic Recombination Layers. <i>Journal of Physical Chemistry C</i> , 2017, 121, 27256-27262.	3.1	40
278	Solar Cell Efficiency Tables. <i>ChemistryViews</i> , 0, , .	0.0	40
279	Phonon lifetimes in model quantum dot superlattice systems with applications to the hot carrier solar cell. <i>Solar Energy Materials and Solar Cells</i> , 2010, 94, 1931-1935.	6.2	39
280	Size controlled synthesis of Ge nanocrystals in SiO ₂ at temperatures below 400°C using magnetron sputtering. <i>Applied Physics Letters</i> , 2010, 96, 261901.	3.3	39
281	Re-evaluation of literature values of silver optical constants. <i>Optics Express</i> , 2015, 23, 2133.	3.4	39
282	High-efficiency, laser grooved, buried contact silicon solar cells. <i>Applied Physics Letters</i> , 1988, 52, 407-409.	3.3	38
283	From junction to terminal: Extended reciprocity relations in solar cell operation. <i>Physical Review B</i> , 2012, 85, .	3.2	38
284	Solar cell minority carrier lifetime using open-circuit voltage decay. <i>Solar Cells</i> , 1984, 11, 147-161.	0.6	37
285	Investigation of polycrystalline silicon deposition on glass substrates. <i>Solar Energy Materials and Solar Cells</i> , 1993, 31, 51-60.	6.2	37
286	Optical gain in materials with indirect transitions. <i>Journal of Applied Physics</i> , 2003, 93, 9058-9061.	2.5	37
287	Fabrication of multilayered Ge nanocrystals by magnetron sputtering and annealing. <i>Nanotechnology</i> , 2008, 19, 455611.	2.6	37
288	In situ low temperature growth of poly-crystalline germanium thin film on glass by RF magnetron sputtering. <i>Solar Energy Materials and Solar Cells</i> , 2010, 94, 1501-1505.	6.2	37

#	ARTICLE	IF	CITATIONS
289	Limiting photovoltaic efficiency under new ASTM International G173â€based reference spectra. Progress in Photovoltaics: Research and Applications, 2012, 20, 954-959.	8.1	37
290	A novel silver nanoparticle assisted texture as broadband antireflection coating for solar cell applications. Solar Energy Materials and Solar Cells, 2013, 109, 233-239.	6.2	37
291	Experimental Assessment of Temperature Coefficient Theories for Silicon Solar Cells. IEEE Journal of Photovoltaics, 2016, 6, 56-60.	2.5	37
292	Self-assembled Nanometer-Scale ZnS Structure at the CZTS/ZnCdS Heterointerface for High-Efficiency Wide Band Gap Cu ₂ ZnSnS ₄ Solar Cells. Chemistry of Materials, 2018, 30, 4008-4016.	6.7	37
293	Synergistic effect of potassium and iodine from potassium triiodide complex additive on gas-quenched perovskite solar cells. Nano Energy, 2019, 63, 103853.	16.0	37
294	Impact of microstructure on the electronâ€hole interaction in lead halide perovskites. Energy and Environmental Science, 2017, 10, 1358-1366.	30.8	36
295	Enhancement of Schottky solar cell efficiency above its semiempirical limit. Applied Physics Letters, 1975, 27, 287-288.	3.3	35
296	Correlation between currentâ€voltage and capacitanceâ€voltage Schottky barrier height on (100) and (110) GaAs and (110) InP surfaces. Journal of Applied Physics, 1990, 68, 3470-3474.	2.5	35
297	Crystalline Silicon Photovoltaic Cells. Advanced Materials, 2001, 13, 1019-1022.	21.0	35
298	Improved value for the silicon free exciton binding energy. AIP Advances, 2013, 3, .	1.3	35
299	Recombination saturation effects in silicon solar cells. IEEE Transactions on Electron Devices, 1994, 41, 1556-1569.	3.0	34
300	Correlation between stress and carrier nonradiative recombination for silicon nanocrystals in an oxide matrix. Nanotechnology, 2011, 22, 335703.	2.6	34
301	The effect of thermal evaporated MoO ₃ intermediate layer as primary back contact for kesterite Cu ₂ ZnSnS ₄ solar cells. Thin Solid Films, 2018, 648, 39-45.	1.8	34
302	Electrode Design to Overcome Substrate Transparency Limitations for Highly Efficient 1 cm ² Mesoscopic Perovskite Solar Cells. Joule, 2018, 2, 2694-2705.	24.0	34
303	Minority carrier lifetimes using compensated differential open circuit voltage decay. Solid-State Electronics, 1983, 26, 1117-1122.	1.4	33
304	Solar cell efficiency tables (version 3). Progress in Photovoltaics: Research and Applications, 1994, 2, 27-34.	8.1	33
305	Surface passivation in high efficiency silicon solar cells. Solar Energy Materials and Solar Cells, 2001, 65, 377-384.	6.2	33
306	Analytical expressions for spectral composition of band photoluminescence from silicon wafers and bricks. Applied Physics Letters, 2011, 99, 131112.	3.3	33

#	ARTICLE	IF	CITATIONS
307	Recent Advances in Silicon Solar Cell Performance. , 1991, , 250-253.		33
308	Bounds upon grain boundary effects in minority carrier semiconductor devices: A rigorous $\hat{\epsilon}$ -perturbation approach with application to silicon solar cells. Journal of Applied Physics, 1996, 80, 1515-1521.	2.5	32
309	Effect of substrate heating on the adhesion and humidity resistance of evaporated MgF ₂ /ZnS antireflection coatings and on the performance of high-efficiency silicon solar cells. Solar Energy Materials and Solar Cells, 1998, 51, 393-400.	6.2	32
310	Solar cell efficiency tables(version 24). Progress in Photovoltaics: Research and Applications, 2004, 12, 365-372.	8.1	32
311	Exploring the application of metastable wurtzite nanocrystals in pure-sulfide Cu ₂ ZnSnS ₄ solar cells by forming nearly micron-sized large grains. Journal of Materials Chemistry A, 2015, 3, 23185-23193.	10.3	32
312	Accurate expressions for solar cell fill factors including series and shunt resistances. Applied Physics Letters, 2016, 108, .	3.3	32
313	Systematic Efficiency Improvement for Cu ₂ ZnSn(S,Se) ₄ Solar Cells By Double Cation Incorporation with Cd and Ge. Advanced Functional Materials, 2021, 31, 2104528.	14.9	32
314	Solar cell efficiency tables (version 19). Progress in Photovoltaics: Research and Applications, 2002, 10, 55-61.	8.1	31
315	Solar cell efficiency tables(version 23). Progress in Photovoltaics: Research and Applications, 2004, 12, 55-62.	8.1	31
316	Scaling limits to large area perovskite solar cell efficiency. Progress in Photovoltaics: Research and Applications, 2018, 26, 659-674.	8.1	31
317	The future of crystalline silicon solar cells. Progress in Photovoltaics: Research and Applications, 2000, 8, 127-139.	8.1	30
318	Interpretation of the Commonly Observed I-V Characteristics of C-Si Cells Having Ideality Factor Larger Than Two. , 2006, , .		30
319	Comparison of DLIT- and PL-based Local Solar Cell Efficiency Analysis. Energy Procedia, 2013, 38, 2-12.	1.8	30
320	Improved modeling of photoluminescent and electroluminescent coupling in multijunction solar cells. Solar Energy Materials and Solar Cells, 2015, 143, 48-51.	6.2	30
321	The Impact of parasitic loss on solar cells with plasmonic nano-textured rear reflectors. Scientific Reports, 2017, 7, 12826.	3.3	30
322	Current transport mechanisms studied by I-V-T and IR photoemission measurements on a P-doped PtSi Schottky diode. Solid-State Electronics, 1993, 36, 1107-1116.	1.4	29
323	Improved nanocrystal formation, quantum confinement and carrier transport properties of doped Si quantum dot superlattices for third generation photovoltaics. Progress in Photovoltaics: Research and Applications, 2013, 21, 569-577.	8.1	29
324	Kinetics of light-induced degradation in semi-transparent perovskite solar cells. Solar Energy Materials and Solar Cells, 2021, 219, 110776.	6.2	29

#	ARTICLE	IF	CITATIONS
325	Rear surface passivation of high efficiency silicon solar cells by a floating junction. Journal of Applied Physics, 1996, 80, 3574-3586.	2.5	28
326	Improved efficiency silicon solar cell module. IEEE Electron Device Letters, 1997, 18, 48-50.	3.9	28
327	Solar cell efficiency tables (version 14). Progress in Photovoltaics: Research and Applications, 1999, 7, 321-326.	8.1	28
328	Resonant tunneling through defects in an insulator: Modeling and solar cell applications. Journal of Applied Physics, 2004, 96, 5006-5012.	2.5	28
329	Impacts of Post-metallisation Processes on the Electrical and Photovoltaic Properties of Si Quantum Dot Solar Cells. Nanoscale Research Letters, 2010, 5, 1762-1767.	5.7	28
330	Corrigendum to "Solar cell efficiency tables (version 49)" [Prog. Photovolt: Res. Appl. 2017; 25:333-334]. Progress in Photovoltaics: Research and Applications, 2017, 25, 333-334.	8.1	28
331	The depletion layer collection efficiency for a junction, Schottky diode, and surface insulator solar cells. Journal of Applied Physics, 1976, 47, 547-554.	2.5	27
332	678 mV open circuit voltage silicon solar cells. Applied Physics Letters, 1981, 39, 483-485.	3.3	27
333	High-efficiency optical emission, detection, and coupling using silicon diodes. Journal of Applied Physics, 2002, 92, 2977-2979.	2.5	27
334	Investigation of boron antimonide as hot carrier absorber material. Solar Energy Materials and Solar Cells, 2013, 111, 123-126.	6.2	27
335	Electro- and photoluminescence imaging as fast screening technique of the layer uniformity and device degradation in planar perovskite solar cells. Journal of Applied Physics, 2016, 120, .	2.5	27
336	Boosting the kesterite Cu ₂ ZnSnS ₄ solar cells performance by diode laser annealing. Solar Energy Materials and Solar Cells, 2018, 175, 71-76.	6.2	27
337	Solar cell efficiency tables (version 2). Progress in Photovoltaics: Research and Applications, 1993, 1, 225-227.	8.1	26
338	Solar cell efficiency tables (version 26). Progress in Photovoltaics: Research and Applications, 2005, 13, 387-392.	8.1	26
339	Impact of interface on the effective band gap of Si quantum dots. Solar Energy Materials and Solar Cells, 2009, 93, 753-758.	6.2	26
340	Size dependent optical properties of Si quantum dots in Si-rich nitride/Si ₃ N ₄ superlattice synthesized by magnetron sputtering. Journal of Applied Physics, 2011, 109, .	2.5	26
341	Study of sputtered Cu ₂ ZnSnS ₄ thin films on Si. Applied Surface Science, 2018, 459, 700-706.	6.1	26
342	High open circuit voltage CuSbS ₂ solar cells achieved through the formation of epitaxial growth of CdS/CuSbS ₂ hetero interface by post annealing treatment. Progress in Photovoltaics: Research and Applications, 2019, 27, 37-43.	8.1	26

#	ARTICLE	IF	CITATIONS
343	Characteristics of p-type PtSi Schottky diodes under reverse bias. Journal of Applied Physics, 1990, 68, 4127-4132.	2.5	25
344	Solar cell efficiency tables (version 8). Progress in Photovoltaics: Research and Applications, 1996, 4, 321-325.	8.1	25
345	Antireflection and surface passivation behaviour of SiO ₂ /Si/SiO ₂ quantum wells on silicon. Solar Energy Materials and Solar Cells, 2002, 74, 147-154.	6.2	25
346	Solar cell efficiency tables (version 21). Progress in Photovoltaics: Research and Applications, 2003, 11, 39-45.	8.1	25
347	Learning experience for thin-film solar modules: First Solar, Inc. case study. Progress in Photovoltaics: Research and Applications, 2011, 19, 498-500.	8.1	25
348	Sentaurus modelling of 6.9% Cu ₂ ZnSnS ₄ device based on comprehensive electrical & optical characterization. Solar Energy Materials and Solar Cells, 2017, 160, 372-381.	6.2	25
349	Tracking solar cell conversion efficiency. Nature Reviews Physics, 2020, 2, 172-173.	26.6	25
350	Doping of Silicon Quantum Dots Embedded in Nitride Matrix for All-Silicon Tandem Cells. Japanese Journal of Applied Physics, 2012, 51, 10NE10.	1.5	25
351	Large-Grain Spanning Monolayer Cu ₂ ZnSnSe ₄ Thin-Film Solar Cells Grown from Metal Precursor. Small, 2022, 18, e2105044.	10.0	25
352	Solar cell efficiency tables (version 4). Progress in Photovoltaics: Research and Applications, 1994, 2, 231-234.	8.1	24
353	High-resolution stress assessments of interconnect/dielectric electronic patterns using optically active point defects of silica glass as a stress sensor. Journal of Applied Physics, 2007, 101, 093514.	2.5	24
354	Intermediate Layer Development for Laser-Crystallized Thin-Film Silicon Solar Cells on Glass. IEEE Journal of Photovoltaics, 2015, 5, 9-16.	2.5	24
355	Rapid thermal annealed Molybdenum back contact for Cu ₂ ZnSnS ₄ thin film solar cells. Applied Physics Letters, 2015, 106, .	3.3	24
356	Solar cell efficiency tables (version 7). Progress in Photovoltaics: Research and Applications, 1996, 4, 59-62.	8.1	23
357	Solar Cell Efficiency Tables (Version 9). Progress in Photovoltaics: Research and Applications, 1997, 5, 51-54.	8.1	23
358	Effects of non-ideal energy selective contacts and experimental carrier cooling rate on the performance of an indium nitride based hot carrier solar cell. Applied Physics Letters, 2011, 99, .	3.3	23
359	Optical Probe Ion and Carrier Dynamics at the CH ₃ NH ₃ PbI ₃ Interface with Electron and Hole Transport Materials. Advanced Materials Interfaces, 2016, 3, 1600467.	3.7	23
360	Low-Temperature Solution Processed Random Silver Nanowire as a Promising Replacement for Indium Tin Oxide. ACS Applied Materials & Interfaces, 2017, 9, 34093-34100.	8.0	23

#	ARTICLE	IF	CITATIONS
361	Combatting temperature and reverse-bias challenges facing perovskite solar cells. <i>Joule</i> , 2022, 6, 1782-1797.	24.0	23
362	Accelerated publication 23.5% efficient silicon solar cell. <i>Progress in Photovoltaics: Research and Applications</i> , 1994, 2, 227-230.	8.1	22
363	22.7% efficient silicon photovoltaic modules with textured front surface. <i>IEEE Transactions on Electron Devices</i> , 1999, 46, 1495-1497.	3.0	22
364	Performance degradation in CZ(B) cells and improved stability high efficiency PERT and PERL silicon cells on a variety of SEH MCZ(B), FZ(B) and CZ(Ga) substrates. <i>Progress in Photovoltaics: Research and Applications</i> , 2000, 8, 549-558.	8.1	22
365	Improved local efficiency imaging via photoluminescence for silicon solar cells. <i>Solar Energy Materials and Solar Cells</i> , 2014, 123, 41-46.	6.2	22
366	Cyclic thermal annealing on Ge/Si(100) epitaxial films grown by magnetron sputtering. <i>Thin Solid Films</i> , 2015, 574, 99-102.	1.8	22
367	Defect-Resolved Effective Majority Carrier Mobility in Highly Anisotropic Antimony Chalcogenide Thin-Film Solar Cells. <i>Solar Rrl</i> , 2021, 5, 2000693.	5.8	22
368	Impurity photovoltaic effect with defect relaxation: Implications for low band gap semiconductors such as silicon. <i>Journal of Applied Physics</i> , 2004, 96, 2603-2609.	2.5	21
369	Electrical properties of conductive Ge nanocrystal thin films fabricated by low temperature <i>in situ</i> growth. <i>Nanotechnology</i> , 2011, 22, 125204.	2.6	21
370	Improvement of Cs _{0.85} (FAPbI ₃) _{0.15} (MAPbBr ₃) _{0.15} Quality Via DMSO-Molecule-Control to Increase the Efficiency and Boost the Long-Term Stability of 1-µm ² Sized Planar Perovskite Solar Cells. <i>Solar Rrl</i> , 2019, 3, 1800338.	5.8	21
371	Solar cell efficiency tables (version 10). <i>Progress in Photovoltaics: Research and Applications</i> , 1997, 5, 265-268.	8.1	20
372	Solar cell efficiency tables (version 13). <i>Progress in Photovoltaics: Research and Applications</i> , 1999, 7, 31-37.	8.1	20
373	Quantitative evaluation of boron-induced disorder in multilayers containing silicon nanocrystals in an oxide matrix designed for photovoltaic applications. <i>Optics Express</i> , 2010, 18, 22004.	3.4	20
374	Three-dimensional imaging for precise structural control of Si quantum dot networks for all-Si solar cells. <i>Nanoscale</i> , 2013, 5, 7499.	5.6	20
375	Defect annealing in ultra-thin polycrystalline silicon films on glass: Rapid thermal versus laser processing. <i>Materials Letters</i> , 2013, 107, 1-4.	2.6	20
376	Micro-structural defects in polycrystalline silicon thin-film solar cells on glass by solid-phase crystallisation and laser-induced liquid-phase crystallisation. <i>Solar Energy Materials and Solar Cells</i> , 2015, 132, 282-288.	6.2	20
377	Light-Bias-Dependent External Quantum Efficiency of Kesterite Cu ₂ ZnSnS ₄ Solar Cells. <i>ACS Photonics</i> , 2017, 4, 1684-1690.	6.6	20
378	The efficiency of grating solar cells. <i>Journal of Applied Physics</i> , 1978, 49, 437-442.	2.5	19

#	ARTICLE	IF	CITATIONS
379	Double layer antireflection coating for high-efficiency passivated emitter silicon solar cells. IEEE Transactions on Electron Devices, 1994, 41, 1592-1594.	3.0	19
380	Junction recombination current in abrupt junction diodes under forward bias. Journal of Applied Physics, 1996, 80, 3083-3090.	2.5	19
381	16.4% efficient, thin active layer silicon solar cell grown by liquid phase epitaxy. Solar Energy Materials and Solar Cells, 1996, 40, 231-238.	6.2	19
382	Excitation dependence of photoluminescence in silicon quantum dots. New Journal of Physics, 2007, 9, 337-337.	2.9	19
383	Designing Bottom Silicon Solar Cells for Multijunction Devices. IEEE Journal of Photovoltaics, 2015, 5, 683-690.	2.5	19
384	9.6%-Efficient all-inorganic Sb ₂ (S,Se) ₃ solar cells with a MnS hole-transporting layer. Journal of Materials Chemistry A, 2022, 10, 2835-2841.	10.3	19
385	Minority carrier mobility of Czochralski-grown silicon by microwave-detected photoconductance decay. Journal of Applied Physics, 1993, 74, 6212-6216.	2.5	18
386	Decreased emitter sheet resistivity loss in high-efficiency silicon solar cells. Progress in Photovoltaics: Research and Applications, 1994, 2, 3-17.	8.1	18
387	Two new efficient crystalline silicon light-trapping textures. Progress in Photovoltaics: Research and Applications, 1999, 7, 317-320.	8.1	18
388	Solar cell efficiency tables (version 16). Progress in Photovoltaics: Research and Applications, 2000, 8, 377-383.	8.1	18
389	Large Grained, Low Defect Density Polycrystalline Silicon on Glass Substrates by Large-area Diode Laser Crystallisation. Materials Research Society Symposia Proceedings, 2012, 1426, 251-256.	0.1	18
390	The roles of shallow and deep levels in the recombination behavior of polycrystalline silicon on glass solar cells. Progress in Photovoltaics: Research and Applications, 2012, 20, 915-922.	8.1	18
391	Full Spectrum Photoluminescence Lifetime Analyses on Silicon Bricks. IEEE Journal of Photovoltaics, 2013, 3, 962-969.	2.5	18
392	Revealing Dynamic Effects of Mobile Ions in Halide Perovskite Solar Cells Using Time-Resolved Microspectroscopy. Small Methods, 2021, 5, e2000731.	8.6	18
393	Photocurrent loss within the depletion region of polycrystalline solar cells. Solid-State Electronics, 1978, 21, 1139-1144.	1.4	17
394	Oxidation condition dependence of surface passivation in high efficiency silicon solar cells. Applied Physics Letters, 1985, 47, 818-820.	3.3	17
395	20% efficient photovoltaic module. IEEE Electron Device Letters, 1993, 14, 539-541.	3.9	17
396	Solar cell efficiency tables (version 5). Progress in Photovoltaics: Research and Applications, 1995, 3, 51-55.	8.1	17

#	ARTICLE	IF	CITATIONS
397	Fabrication and characterization of tin-based nanocrystals. Journal of Applied Physics, 2007, 102, 114304.	2.5	17
398	Influence of hydrogen on structural and optical properties of low temperature polycrystalline Ge films deposited by RF magnetron sputtering. Journal of Crystal Growth, 2010, 312, 2647-2655.	1.5	17
399	Improved silicon optical parameters at 25°C, 295K and 300K including temperature coefficients. Progress in Photovoltaics: Research and Applications, 2022, 30, 164-179.	8.1	17
400	Low-temperature liquid phase epitaxy of silicon. Materials Letters, 1991, 12, 339-343.	2.6	16
401	Band edge optical absorption in intrinsic silicon: Assessment of the indirect transition and disorder models. Journal of Applied Physics, 1993, 73, 3988-3996.	2.5	16
402	CRYSTALLINE SILICON SOLAR CELLS. Series on Photoconversion of Solar Energy, 2001, , 149-197.	0.2	16
403	Study of silicon quantum dots in a SiO ₂ matrix for energy selective contacts applications. Solar Energy Materials and Solar Cells, 2010, 94, 1936-1941.	6.2	16
404	In situ growth of Ge-rich poly-SiGe:H thin films on glass by RF magnetron sputtering for photovoltaic applications. Applied Surface Science, 2011, 257, 4354-4359.	6.1	16
405	Spatially resolved photoluminescence imaging of essential silicon solar cell parameters. , 2012, , .		16
406	Results from coupled optical and electrical sentaurus TCAD models of a gallium phosphide on silicon electron carrier selective contact solar cell. , 2014, , .		16
407	Luminescence Imaging Characterization of Perovskite Solar Cells: A Note on the Analysis and Reporting the Results. Advanced Energy Materials, 2018, 8, 1702256.	19.5	16
408	Solar cell efficiency tables (version 6). Progress in Photovoltaics: Research and Applications, 1995, 3, 229-233.	8.1	15
409	Photoluminescence in crystalline silicon quantum wells. Journal of Applied Physics, 2007, 101, 024321.	2.5	15
410	N-type conductivity of nanostructured thin film composed of antimony-doped Si nanocrystals in silicon nitride matrix. Europhysics Letters, 2011, 96, 17011.	2.0	15
411	Intermediate Layers for Thin-Film Polycrystalline Silicon Solar Cells on Glass Formed by Diode Laser Crystallization. Materials Research Society Symposia Proceedings, 2012, 1426, 63-68.	0.1	15
412	Photoluminescence based open circuit voltage and effective lifetime images re-interpretation for solar cells: The influence of horizontal balancing currents. Solar Energy Materials and Solar Cells, 2014, 130, 393-396.	6.2	15
413	Epitaxial growth of single-crystalline silicon-germanium on silicon by aluminium-assisted crystallization. Scripta Materialia, 2014, 71, 25-28.	5.2	15
414	Radio frequency magnetron sputtered epitaxial Cu ₂ ZnSnS ₄ thin film on ZnS(100). Physica Status Solidi - Rapid Research Letters, 2014, 8, 404-407.	2.4	15





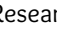




#	ARTICLE	IF	CITATIONS
415	Self-Assembled Nanostructured Rear Reflector Designs for Thin-Film Solar Cells. ACS Photonics, 2015, 2, 1108-1116.	6.6	15
416	Simplified technique for calculating mismatch loss in mass production. Solar Energy Materials and Solar Cells, 2015, 134, 236-243.	6.2	15
417	Photoluminescent and electroluminescent couplings in monolithic tandem solar cells. Progress in Photovoltaics: Research and Applications, 2016, 24, 1566-1576.	8.1	15
418	Enhancement of MIS solar cell efficiency by peripheral collection. Applied Physics Letters, 1977, 31, 705-707.	3.3	14
419	Atomistic structure of SiO ₂ •Si•SiO ₂ quantum wells with an apparently crystalline silicon oxide. Journal of Applied Physics, 2004, 96, 3211-3216.	2.5	14
420	High external quantum efficiency of planar semiconductor structures. Semiconductor Science and Technology, 2004, 19, 1232-1235.	2.0	14
421	SHORT COMMUNICATION: Price/efficiency correlations for 2004 photovoltaic modules. Progress in Photovoltaics: Research and Applications, 2005, 13, 85-87.	8.1	14
422	Recent Developments and Future Prospects for Third Generation and Other Advanced Cells. , 2006, , .		14
423	Rare materials for photovoltaics: Recent tellurium price fluctuations and availability from copper refining. Solar Energy Materials and Solar Cells, 2013, 119, 256-260.	6.2	14
424	Silicon wafer-based tandem cells: The ultimate photovoltaic solution?. Proceedings of SPIE, 2014, , .	0.8	14
425	Equivalent circuit analysis of radiative coupling in monolithic tandem solar cells. Applied Physics Letters, 2015, 106, .	3.3	14
426	Time-resolved fluorescence anisotropy study of organic lead halide perovskite. Solar Energy Materials and Solar Cells, 2016, 151, 102-112.	6.2	14
427	Hybrid Ag Nanowire•ITO as Transparent Conductive Electrode for Pure Sulfide Kesterite Cu ₂ ZnSnS ₄ Solar Cells. Journal of Physical Chemistry C, 2017, 121, 20597-20604.	3.1	14
428	Passive PV module cooling under free convection through vortex generators. Renewable Energy, 2022, 190, 319-329.	8.9	14
429	Electrostatic effects in inversion layer metal•insulator•semiconductor solar cells. Applied Physics Letters, 1980, 37, 1087-1089.	3.3	13
430	Evaluation of binary and ternary melts for the low temperature liquid phase epitaxial growth of silicon. Journal of Electronic Materials, 1991, 20, 635-641.	2.2	13
431	717•mV open•circuit voltage silicon solar cells using hole•constrained surface passivation. Applied Physics Letters, 1994, 64, 199-201.	3.3	13
432	Two-dimensional numerical simulations of high-efficiency silicon solar cells. Microelectronics Journal, 1995, 26, 273-286.	2.0	13

#	ARTICLE	IF	CITATIONS
433	The effects of solvent and dopant impurities on the performance of LPE silicon solar cells. <i>Solar Energy Materials and Solar Cells</i> , 1996, 41-42, 53-60.	6.2	13
434	High-efficiency Multicrystalline Silicon Solar Cells using Standard High-temperature, Float-zoned Cell Processing. <i>Progress in Photovoltaics: Research and Applications</i> , 1997, 5, 169-174.	8.1	13
435	Depletion region recombination in silicon thin-film multilayer solar cells. <i>Progress in Photovoltaics: Research and Applications</i> , 1996, 4, 375-380.	8.1	13
436	Modeling and optimization of thin-film devices with Si/sub 1-x/Ge/sub x/ alloys. <i>IEEE Transactions on Electron Devices</i> , 1999, 46, 2111-2115.	3.0	13
437	High external quantum efficiency from double heterostructure InGaP/GaAs layers as selective emitters for thermophotonic systems. <i>Semiconductor Science and Technology</i> , 2004, 19, 1268-1272.	2.0	13
438	Ultrafast carrier dynamics of Si quantum dots embedded in SiN matrix. <i>Applied Physics Letters</i> , 2007, 90, 081105.	3.3	13
439	Anomalous temperature dependence of diode saturation currents in polycrystalline silicon thin-film solar cells on glass. <i>Journal of Applied Physics</i> , 2009, 105, 103705.	2.5	13
440	Characterisation of size-controlled and red luminescent Ge nanocrystals in multilayered superlattice structure. <i>Thin Solid Films</i> , 2010, 518, 5483-5487.	1.8	13
441	Optical characterisation of silicon nanocrystals embedded in SiO ₂ /Si ₃ N ₄ hybrid matrix for third generation photovoltaics. <i>Nanoscale Research Letters</i> , 2011, 6, 612.	5.7	13
442	Ideal solar cell equation in the presence of photon recycling. <i>Journal of Applied Physics</i> , 2014, 116, .	2.5	13
443	Optical modelling data for room temperature optical properties of organic-inorganic lead halide perovskites. <i>Data in Brief</i> , 2015, 3, 201-208.	1.0	13
444	Diode laser annealing on Ge/Si (100) epitaxial films grown by magnetron sputtering. <i>Thin Solid Films</i> , 2016, 609, 49-52.	1.8	13
445	Low-pressure accessible gas-quenching for absolute methylammonium-free perovskite solar cells. <i>Journal of Materials Chemistry A</i> , 2022, 10, 2105-2112.	10.3	13
446	17.6% efficient multilayer thin-film silicon solar cells deposited on heavily doped silicon substrates. <i>Progress in Photovoltaics: Research and Applications</i> , 1996, 4, 369-373.	8.1	12
447	Evidence for generalized Kirchhoff's law from angle-resolved electroluminescence of high efficiency silicon solar cells. <i>Applied Physics Letters</i> , 2004, 85, 2484-2486.	3.3	12
448	Analytical treatment of Trivich's Flinn and Shockley's Queisser photovoltaic efficiency limits using polylogarithms. <i>Progress in Photovoltaics: Research and Applications</i> , 2012, 20, 127-134.	8.1	12
449	Optimisation of the Back Surface Reflector for Textured Polycrystalline Si Thin Film Solar Cells. <i>Energy Procedia</i> , 2013, 33, 118-128.	1.8	12
450	Extraction of black hole coalescence waveforms from noisy data. <i>Physics Letters, Section B: Nuclear, Elementary Particle and High-Energy Physics</i> , 2018, 784, 312-323.	4.1	12

#	ARTICLE	IF	CITATIONS
451	Singlet fission and tandem solar cells reduce thermal degradation and enhance lifespan. Progress in Photovoltaics: Research and Applications, 2021, 29, 899-906.	8.1	12
452	Event Report. Brain Sport: The 1996 World Solar Challenge Solar Car Race Across Australia. Progress in Photovoltaics: Research and Applications, 1997, 5, 69-76.	8.1	11
453	Accelerated publication?? a new initiative. Progress in Photovoltaics: Research and Applications, 2005, 13, 1-2.	8.1	11
454	Structural inhomogeneities in polycrystalline silicon on glass solar cells and their effects on device characteristics. Progress in Photovoltaics: Research and Applications, 2011, 19, 695-705.	8.1	11
455	A holistic review of mismatch loss: From manufacturing decision making to losses in fielded arrays. Solar Energy Materials and Solar Cells, 2018, 174, 214-224.	6.2	11
456	Design of an intermediate Bragg reflector within triple-junction solar cells for spectrum splitting applications. Solar Energy Materials and Solar Cells, 2019, 193, 259-269.	6.2	11
457	Optical and Thermal Emission Benefits of Differently Textured Glass for Photovoltaic Modules. IEEE Journal of Photovoltaics, 2021, 11, 131-137.	2.5	11
458	Low-Cost Fabrication of Sb_2S_3 Solar Cells: Direct Evaporation from Raw Stibnite Ore. Solar Rrl, 2022, 6, .	5.8	11
459	The short-wavelength response of MIS solar cells. Journal of Applied Physics, 1979, 50, 1116-1122.	2.5	10
460	Thin semiconducting layers and nanostructures as active and passive emitters for thermophotonics and thermophotovoltaics. Physica E: Low-Dimensional Systems and Nanostructures, 2002, 14, 91-95.	2.7	10
461	Near-band edge light emission from silicon semiconductor on insulator diodes. Applied Physics Letters, 2004, 85, 2830-2832.	3.3	10
462	Impact of bridge- and double-bonded oxygen on OH-terminated Si quantum dots: A density-functional-Hartree-Fock study. Materials Science and Engineering B: Solid-State Materials for Advanced Technology, 2009, 159-160, 117-121.	3.5	10
463	Surface states induced high P-type conductivity in nanostructured thin film composed of Ge nanocrystals in SiO ₂ matrix. Applied Physics Letters, 2010, 97, 132109.	3.3	10
464	Single layer of silicon quantum dots in silicon oxide matrix: Investigation of forming gas hydrogenation on photoluminescence properties and study of the composition of silicon rich oxide layers. Journal of Crystal Growth, 2011, 327, 84-88.	1.5	10
465	One-step aluminium-assisted crystallization of Ge epitaxy on Si by magnetron sputtering. Applied Physics Letters, 2014, 104, 052107.	3.3	10
466	Grain boundary effects on the optical constants and Drude relaxation times of silver films. Journal of Applied Physics, 2016, 120, .	2.5	10
467	Immediate and Temporal Enhancement of Power Conversion Efficiency in Surface-Passivated Perovskite Solar Cells. ACS Applied Materials & Interfaces, 2021, 13, 39178-39185.	8.0	10
468	Crystalline and polycrystalline silicon tandem junction solar cells: Theoretical advantages. Solar Cells, 1986, 18, 31-40.	0.6	9

#	ARTICLE	IF	CITATIONS
469	Two-dimensional minority carrier flow in high-efficiency silicon solar cells at short-circuit, open-circuit and maximum power point operating conditions. <i>Solar Energy Materials and Solar Cells</i> , 1994, 34, 149-160.	6.2	9
470	World solar challenge 1993: The trans-australian solar car race. <i>Progress in Photovoltaics: Research and Applications</i> , 1994, 2, 73-79.	8.1	9
471	Solar cell efficiency tables (version 12). <i>Progress in Photovoltaics: Research and Applications</i> , 1998, 6, 265-270.	8.1	9
472	Structural and optical study of Ge nanocrystals embedded in Si ₃ N ₄ matrix. <i>Energy Procedia</i> , 2011, 10, 20-27.	1.8	9
473	Surface plasmons for improving the performance of quantum dot structures for third generation solar cell applications. <i>Physica Status Solidi C: Current Topics in Solid State Physics</i> , 2011, 8, 181-184.	0.8	9
474	Hot Carrier solar cell absorbers: Superstructures, materials and mechanisms for slowed carrier cooling. , 2012, , .		9
475	Transient photoconductance and photoluminescence from thick silicon wafers and bricks: Analytical solutions. <i>Solar Energy Materials and Solar Cells</i> , 2013, 111, 189-192.	6.2	9
476	Analytical expressions for spectral composition of band luminescence from silicon solar cells under optical and electrical bias. <i>Applied Physics Letters</i> , 2014, 104, .	3.3	9
477	Extended spectral response analysis of conventional and front surface field solar cells. <i>Solar Energy Materials and Solar Cells</i> , 2015, 134, 346-350.	6.2	9
478	Grain Quality Engineering for Organic Metal Halide Perovskites Using Mixed Antisolvent Spraying Treatment. <i>Solar Rrl</i> , 2020, 4, 1900397.	5.8	9
479	Sublinear current response in high-efficiency, high-resistivity silicon solar cells: Theory and experiment. <i>Applied Physics Letters</i> , 1988, 52, 1361-1363.	3.3	8
480	An optimized prismatic cover design for concentrator and nonconcentrator solar cells. <i>Journal of Applied Physics</i> , 1990, 68, 1345-1350.	2.5	8
481	A note on current-voltage measurements of n-type and p-type Pd ₂ Si Schottky diodes. <i>Solid-State Electronics</i> , 1991, 34, 215-216.	1.4	8
482	Plasma-grooved, buried contact silicon solar cells. <i>Journal of Applied Physics</i> , 1991, 69, 4135-4136.	2.5	8
483	<i>In situ</i> formation of tin nanocrystals embedded in silicon nitride matrix. <i>Journal of Applied Physics</i> , 2009, 105, .	2.5	8
484	Lateral growth of Ge nanocrystals in a thin Ge-rich silicon nitride layer. <i>Journal of Crystal Growth</i> , 2013, 383, 36-42.	1.5	8
485	High-voltage p-type PERC solar cells with anchored plating and hydrogenation. <i>Progress in Photovoltaics: Research and Applications</i> , 2018, 26, 397-401.	8.1	8
486	Deconstruction-assisted perovskite formation for sequential solution processing of Cs _{0.15} (MA _{0.7} FA _{0.3}) _{0.85} PbI ₃ solar cells. <i>Solar Energy Materials and Solar Cells</i> , 2019, 203, 110200.	6.2	8

#	ARTICLE	IF	CITATIONS
487	The potential and design principle for next-generation spectrum-splitting photovoltaics: Targeting 50% efficiency through built-in filters and generalization of concept. Progress in Photovoltaics: Research and Applications, 2019, 27, 899-904.	8.1	8
488	11.6% Efficient Pure Sulfide Cu(In,Ga)S ₂ Solar Cell through a Cu-Deficient and KCN-Free Process. ACS Applied Energy Materials, 2020, 3, 11974-11980.	5.1	8
489	Experimental bounds on band-gap narrowing set by high open circuit voltage silicon solar cells. Journal of Applied Physics, 1985, 57, 591-599.	2.5	7
490	Recent progress in crystalline and polycrystalline silicon solar cells. Solar Energy Materials and Solar Cells, 1991, 23, 111-116.	0.4	7
491	Technology and economics of three advanced silicon solar cells. Progress in Photovoltaics: Research and Applications, 1998, 6, 169-180.	8.1	7
492	A modified Shockley-Read-Hall theory including radiative transitions. Solid-State Electronics, 2003, 47, 685-689.	1.4	7
493	Hot carrier solar cells: Challenges and recent progress. , 2010, , .		7
494	Investigating polysilicon thin film structural changes during rapid thermal annealing of a thin film crystalline silicon on glass solar cell. Journal of Materials Science: Materials in Electronics, 2010, 21, 994-999.	2.2	7
495	Impact of disorder in double barrier QD structures on energy selectivity investigated by two dimensional effective mass approximation. Energy Procedia, 2010, 2, 213-219.	1.8	7
496	Price and supply constraints on Te and In photovoltaics. , 2010, , .		7
497	Perturbation Theory for Solar Cell Efficiency – Basic Principles. IEEE Transactions on Electron Devices, 2011, 58, 4011-4015.	3.0	7
498	Structural dependence of electrical properties of Ge films prepared by RF magnetron sputtering. Applied Physics A: Materials Science and Processing, 2011, 102, 689-694.	2.3	7
499	Compatibility of glass textures with E-beam evaporated polycrystalline silicon thin-film solar cells. Applied Physics A: Materials Science and Processing, 2013, 111, 935-942.	2.3	7
500	Data mining photovoltaic cell manufacturing data. , 2014, , .		7
501	Diode laser crystallization processes of Si thin-film solar cells on glass. EPJ Photovoltaics, 2014, 5, 55204.	1.6	7
502	Temperature Coefficients of Photovoltaic Devices. , 2017, , 29-74.		7
503	Evidence of Low-Temperature Joints in Silver Nanowire Based Transparent Conducting Layers for Solar Cells. ACS Applied Nano Materials, 2020, 3, 3205-3213.	5.0	7
504	Limiting efficiency of bulk and thin-film silicon solar cells in the presence of surface recombination. Progress in Photovoltaics: Research and Applications, 1999, 7, 327-330.	8.1	7

#	ARTICLE	IF	CITATIONS
505	Defect Engineering for Efficient Cu ₂ ZnSnS ₄ Solar Cells via Moisture-Assisted Post-Deposition Annealing. <i>Advanced Optical Materials</i> , 0, , 2200607.	7.3	7
506	23.6% efficient low resistivity silicon concentrator solar cell. <i>Applied Physics Letters</i> , 1986, 49, 194-195.	3.3	6
507	Silicon solar cells: at the crossroads. <i>Progress in Photovoltaics: Research and Applications</i> , 2000, 8, 443-450.	8.1	6
508	Australian educational and research opportunities arising through rapid growth in the photovoltaic industry. <i>Solar Energy Materials and Solar Cells</i> , 2001, 67, 647-654.	6.2	6
509	In-situ fabrication and characterization of ordered Ge QDs in Si ₃ N ₄ matrix without barrier layers by rf-magnetron sputtering. <i>Applied Surface Science</i> , 2014, 290, 167-171.	6.1	6
510	The ultimate efficiency of organolead halide perovskite solar cells limited by Auger processes. <i>Journal of Materials Research</i> , 2016, 31, 2197-2203.	2.6	6
511	Optimization of solar thermophotovoltaic systems including the thermal balance. , 2016, , .		6
512	High-Efficiency Silicon Solar Cell Concepts. , 2018, , 95-128.		6
513	Epitaxial growth of Cu ₂ ZnSnS ₄ thin film on Si by radio frequency magnetron sputtering. <i>Applied Physics Letters</i> , 2020, 116, 123901.	3.3	6
514	Revealing the Dynamics of the Thermal Reaction between Copper and Mixed Halide Perovskite Solar Cells. <i>ACS Applied Materials & Interfaces</i> , 2022, 14, 20866-20874.	8.0	6
515	Bias and thickness dependence of the infra-red Schottky diode studied by internal photoemission. <i>Solid-State Electronics</i> , 1996, 39, 277-280.	1.4	5
516	Limits to the efficiency of silicon multilayer thin film solar cells. <i>Solar Energy Materials and Solar Cells</i> , 1996, 41-42, 3-17.	6.2	5
517	Thin semiconducting layers as active and passive emitters for thermophotonics and thermophotovoltaics. <i>Solar Energy</i> , 2004, 76, 251-254.	6.1	5
518	Third Generation Photovoltaics: Assessment of progress over the last decade. , 2009, , .		5
519	Capacitance and conductance characteristics of silicon nanocrystal metal-insulator-semiconductor devices. <i>Solid-State Electronics</i> , 2009, 53, 530-539.	1.4	5
520	Modelling of metal-insulator-semiconductor devices featuring a silicon quantum well. <i>Physica E: Low-Dimensional Systems and Nanostructures</i> , 2010, 42, 2211-2217.	2.7	5
521	Structural studies on multilayered Ge nanocrystals embedded in Si. Si  Si        	1.8	5
522	Is sour crude or sour gas a potential source of Se and Te?. <i>Progress in Photovoltaics: Research and Applications</i> , 2011, 19, 991-995.	8.1	5

#	ARTICLE	IF	CITATIONS
523	Optimized resonant tunnelling structures with high conductivity and selectivity. Europhysics Letters, 2011, 96, 57006.	2.0	5
524	Photovoltaic Material Resources. Semiconductors and Semimetals, 2012, , 143-183.	0.7	5
525	Improvement of Mo/Cu ₂ ZnSnS ₄ interface for Cu ₂ ZnSnS ₄ (CZTS) thin film solar cell application. Materials Research Society Symposia Proceedings, 2014, 1638, 1.	0.1	5
526	Fast separation of front and bulk defects via photoluminescence on silicon solar cells. Solar Energy Materials and Solar Cells, 2014, 128, 260-263.	6.2	5
527	24.5% Efficiency silicon PERT cells on MCZ substrates and 24.7% efficiency PERL cells on FZ substrates. Progress in Photovoltaics: Research and Applications, 1999, 7, 471-474.	8.1	5
528	High resolution imaging of the interfacial region in metal-insulator-semiconductor and Schottky diodes. Journal of Applied Physics, 1983, 54, 2885-2887.	2.5	4
529	Study of silicon quantum dot p-n or p-i-n junction devices on c-Si substrate. Optoelectronic and Microelectronic Materials and Devices (COMMAD), Conference on, 2008, , .	0.0	4
530	Structural and photoluminescence properties of superlattice structures consisting of Sn-rich SiO ₂ and stoichiometric SiO ₂ layers. Thin Solid Films, 2011, 520, 641-645.	1.8	4
531	A photovoltaic light trapping estimation method for textured glass based on surface decoupling calculation. Solar Energy Materials and Solar Cells, 2013, 109, 82-90.	6.2	4
532	Limiting efficiencies of GaInP/GaAs/Ge up-conversion systems: Addressing the issue of radiative coupling. Applied Physics Letters, 2016, 109, .	3.3	4
533	In situ X-ray diffraction study on epitaxial growth of Si _x Ge _{1-x} on Si by aluminium-assisted crystallization. Journal of Alloys and Compounds, 2017, 695, 1672-1676.	5.5	4
534	Diode laser annealing of epitaxy Ge on sapphire (0 0 0 1) grown by magnetron sputtering. Materials Letters, 2017, 208, 35-38.	2.6	4
535	Diode laser annealing on sputtered epitaxial Cu ₂ ZnSnS ₄ thin films. Physica Status Solidi - Rapid Research Letters, 2017, 11, 1700033.	2.4	4
536	Pathways towards a 50% efficiency spectrum-splitting photovoltaic system: Application of built-in filters and generalization of concept. Energy Procedia, 2018, 150, 83-86.	1.8	4
537	Luminescence imaging of solar modules in full sunlight using ultranarrow bandpass filters. Progress in Photovoltaics: Research and Applications, 2022, 30, 1115-1121.	8.1	4
538	High Efficiency Bulk Crystalline Silicon Light Emitting Diodes. Materials Research Society Symposia Proceedings, 2002, 744, 1.	0.1	3
539	Conductivity of self-organized silicon quantum dots embedded in silicon dioxide. , 2005, , .		3
540	Correlation between fixed charge and capacitance peaks in silicon nanocrystal metal-insulator-semiconductor devices. Semiconductor Science and Technology, 2010, 25, 045011.	2.0	3

#	ARTICLE	IF	CITATIONS
541	Residual stress study of silicon quantum dot in silicon carbide matrix by Raman measurement. <i>Physica Status Solidi C: Current Topics in Solid State Physics</i> , 2011, 8, 185-188.	0.8	3
542	Design of bottom silicon solar cell for multijunction devices. , 2013, , .		3
543	CRYSTALLINE SILICON SOLAR CELLS. <i>Series on Photoconversion of Solar Energy</i> , 2014, , 87-137.	0.2	3
544	Copper plated contacts for large-scale manufacturing. , 2016, , .		3
545	Large Voc improvement and 9.2% efficient pure sulfide $\text{Cu}_{2\text{ZnSnS}_4}$ solar cells by heterojunction interface engineering. , 2016, , .		3
546	Thermal Issues in Photovoltaics and Existing Solutions. , 2017, , 1-28.		3
547	Up-conversion of sunlight by GaInP/GaAs/Ge cell stacks: Limiting efficiency, practical limitation and comparison with tandem cells. <i>Energy Procedia</i> , 2017, 130, 60-65.	1.8	3
548	Fabrication of low-defect Ge-rich SiGe-on-insulator by continuous-wave diode laser-induced recrystallization. <i>Journal of Alloys and Compounds</i> , 2018, 744, 679-682.	5.5	3
549	Reduction of Threading Dislocation Density in Sputtered Ge/Si(100) Epitaxial Films by Continuous-Wave Diode Laser-Induced Recrystallization. <i>ACS Applied Energy Materials</i> , 2018, 1, 1893-1897.	5.1	3
550	Investigating the effect of silicon thickness on ultra-thin silicon on insulator as a compliant substrate for gallium arsenide heteroepitaxial growth. <i>Thin Solid Films</i> , 2018, 653, 371-376.	1.8	3
551	Understanding the effect of Cadmium alloying in high-efficiency sulphide kesterite $\text{Cu}_2\text{Zn}_x\text{Cd}_{1-x}\text{SnS}_4$ solar cell by PDS and HRSTEM. , 2018, , .		3
552	Efficiency Improvement of High Band Gap $\text{Cu}_2\text{ZnSnS}_4$ Solar Cell Achieved by Silver Incorporation. , 2018, , .		3
553	Peer behaviour boosts recycling. <i>Nature Energy</i> , 2021, 6, 862-863.	39.5	3
554	The open-circuit voltage of vertical-junction solar cells. <i>Journal Physics D: Applied Physics</i> , 1976, 9, L57-L59.	2.8	2
555	Solar cell research and development in Australia. <i>Solar Cells</i> , 1989, 26, 1-11.	0.6	2
556	<title>Fully integrated Schottky array: a new generation of metal silicide infrared detectors</title>. , 1990, 1308, 58.		2
557	Diffusion effects in PtSi Schottky diodes under reverse bias. <i>Journal of Applied Physics</i> , 1991, 69, 3601-3604.	2.5	2
558	Multilayer thin film silicon solar cells. <i>Natural Resources Forum</i> , 1995, 19, 269-273.	3.6	2

#	ARTICLE	IF	CITATIONS
559	Capitalizing on two dimensional minority carrier injection in silicon solar cell design. Solar Energy Materials and Solar Cells, 1996, 41-42, 183-193.	6.2	2
560	Modelling implications of recent silicon bandgap narrowing expressions. Progress in Photovoltaics: Research and Applications, 1997, 5, 261-263.	8.1	2
561	<title>High-efficiency silicon solar cells</title>. , 1999, , .		2
562	High-efficiency silicon light emitting diodes. Physica E: Low-Dimensional Systems and Nanostructures, 2003, 16, 351-358.	2.7	2
563	Two Colour Excitation Up-Conversion Efficiency Enhancement for a Silicon Photovoltaic Device using Er ³⁺ -Doped Phosphors. , 2006, , .		2
564	Effects of silicon nanocrystallite density on the Raman-scattering spectra of silicon quantum dot superlattices. , 2006, , .		2
565	Editorial: crystal-gazing special issue. Progress in Photovoltaics: Research and Applications, 2006, 14, 381-381.	8.1	2
566	Investigating Large Area Fabrication of Silicon Quantum Dots in a Nitride Matrix for Photovoltaic Applications. , 2006, , .		2
567	Effect of annealing temperature on the formation of silicon nanocrystals in a nitride matrix. , 2006, , .		2
568	Ultrafast Transient Grating Spectroscopy in Silicon Quantum Dots. Journal of Nanoscience and Nanotechnology, 2009, 9, 4575-4579.	0.9	2
569	Fabrication and characterisation of silicon quantum dots in SiO ₂ /Si ₃ N ₄ hybrid matrix. , 2010, , .		2
570	Doping of Silicon Quantum Dots Embedded in Nitride Matrix for All-Silicon Tandem Cells. Japanese Journal of Applied Physics, 2012, 51, 10NE10.	1.5	2
571	Structural, mechanical and optical properties of Ge nanocrystals embedded in superlattices fabricated by in situ low temperature annealing. Physica E: Low-Dimensional Systems and Nanostructures, 2012, 45, 207-213.	2.7	2
572	High-Efficiency Silicon Solar Cell Concepts. , 2013, , 87-113.		2
573	Heterogeneous nano-particle array for the realization of the hot carrier solar cell. , 2013, , .		2
574	Growth Mechanism and Surface Structure of Ge Nanocrystals Prepared by Thermal Annealing of Cosputtered GeSiO Ternary Precursor. Journal of Nanomaterials, 2014, 2014, 1-7.	2.7	2
575	Correction to "Morphology and Carrier Extraction Study of Organic-Inorganic Metal Halide Perovskite by One- and Two-Photon Fluorescence Microscopy". Journal of Physical Chemistry Letters, 2014, 5, 4038-4038.	4.6	2
576	Diode laser annealing of CZTS thin film solar cells. , 2015, , .		2

#	ARTICLE	IF	CITATIONS
577	Generalised distributed model of a solar cell: Lateral injection effects and impact on cell design and characterisation. Solar Energy Materials and Solar Cells, 2016, 147, 108-114.	6.2	2
578	A Thermal Model for the Design of Photovoltaic Devices. , 2017, , 75-103.		2
579	Design of Bragg Reflector in GaInP/GaInAs/Ge Triple-junction Solar Cells for Spectrum Splitting Applications. , 2018, , .		2
580	Grain Quality Engineering for Organic Metal Halide Perovskites Using Mixed Antisolvent Spraying Treatment. Solar Rrl, 2020, 4, 2070012.	5.8	2
581	Unveiling the Importance of Precursor Preparation for Highly Efficient and Stable Phenethylammonium-Based Perovskite Solar Cells. Solar Rrl, 2020, 4, 1900463.	5.8	2
582	Status of Crystalline Photovoltaic Technology. , 2000, , 2630-2635.		2
583	24.7% Efficient PERL silicon Solar Cells and Other High Efficiency Solar Cell and Module Research at the University of New South Wales. , 2000, , 165-172.		2
584	Corrigendum to "Improved Silicon Optical Parameters at 25°C, 295K and 300K including Temperature Coefficients" [Prog. Photovolt: Res. Appl. 2022; 30: 164-179]. Progress in Photovoltaics: Research and Applications, 2022, 30, 1144-1145.	8.1	2
585	Solar cells: Future directions. Solar Cells, 1984, 12, 95-97.	0.6	1
586	Full Schottky high density 2-D infrared charge coupled detector array. Solid-State Electronics, 1987, 30, 1341-1343.	1.4	1
587	Improved soldering technique for concentrator solar cells. Solar Cells, 1990, 28, 193-197.	0.6	1
588	Strained Si _{1-x} Ge _x layers grown by low-temperature liquid-phase epitaxy. Materials Letters, 1992, 14, 263-267.	2.6	1
589	High-Efficiency Silicon Solar Cell Concepts. , 2003, , 253-278.		1
590	High-efficiency silicon solar cell concepts. , 2005, , 189-214.		1
591	Fabrication of multilayered Ge nanocrystals embedded in SiO _x GeNy films. Applied Surface Science, 2008, 254, 7527-7530.	6.1	1
592	The Future of Thin Film Solar Cells. , 2008, , 96-101.		1
593	“Third generation” photovoltaics and silicon nanostructures. , 2008, , .		1
594	High-Efficiency Silicon Solar Cell Concepts. , 2012, , 99-128.		1

#	ARTICLE	IF	CITATIONS
595	Selective high concentration doping of boron near absorber contacts of a laser crystallized silicon thin-film solar cell on glass. , 2013, , .		1
596	Cu ₂ ZnSnS ₄ thin film solar cell fabricated by magnetron sputtering and sulfurization. Materials Research Society Symposia Proceedings, 2014, 1638, 1.	0.1	1
597	An overview of the Australian Centre for Advanced Photovoltaics and the Australia-US Institute for Advanced Photovoltaics. Materials Research Society Symposia Proceedings, 2015, 1771, 33-44.	0.1	1
598	Potential performance of "out-of-sequence" multi-junction solar cells: iii-v on virtual ge substrates with active si bottom sub-cell. , 2015, , .		1
599	The design of single-junction GaAs and dual-junction GaAs/Si in the presence of threading dislocation density. , 2015, , .		1
600	Illumination dependent carrier dynamics of CH ₃ NH ₃ PbBr ₃ perovskite. Proceedings of SPIE, 2015, , .	0.8	1
601	Effect of a ZnS intermediate layer on properties of Cu ₂ ZnSnS ₄ films from sputtered Zn/CuSn precursors on Si (100) substrate. , 2016, , .		1
602	Promising hybrid graphene-silver nanowire transparent conductive electrode. , 2016, , .		1
603	Unravelling the mechanism of photo-activated ion dynamics in organic-inorganic perovskites. , 2016, , .		1
604	Australian Photovoltaics Research and Development. ACS Energy Letters, 2016, 1, 516-520.	17.4	1
605	Specificities of the Thermal Behavior of Current and Emerging Photovoltaic Technologies. , 2017, , 105-128.		1
606	Effects of Al thickness on one-step aluminium-assisted crystallization of Ge epitaxy on Si by magnetron sputtering. Materials Letters, 2017, 209, 32-35.	2.6	1
607	Defect Control for 12.5% Efficiency Cu ₂ ZnSnSe ₄ Kesterite Thin-Film Solar Cells by Engineering of Local Chemical Environment. SSRN Electronic Journal, 0, , .	0.4	1
608	High Efficiency Silicon Light Emitting Diodes. , 2003, , 1-10.		1
609	High performance silicon solar cells using low dose phosphorus implants. Nuclear Instruments & Methods in Physics Research, 1981, 191, 51-53.	0.9	0
610	Fabrication of thick narrow electrodes on concentrator solar cells. Journal of Vacuum Science and Technology, 1982, 20, 13-15.	1.9	0
611	Highlights of the Fourth International Photovoltaic Science and Engineering Conference (PVSEC-4). Solar Cells, 1989, 27, 3-10.	0.6	0
612	Silicon Parallel Multilayer Thin Film Solar Cells. Materials Research Society Symposia Proceedings, 1996, 426, 103.	0.1	0

#	ARTICLE	IF	CITATIONS
613	Effects of dielectric overcoating on the absorption enhancement of SOI LEDs with metal island films. , 2005, , .		0
614	Bulk silicon for photonics applications. , 2005, , .		0
615	Spectral Properties and dynamics of carriers in Si quantum dots in SiN matrices. , 2006, , .		0
616	Very High-efficiency in Silico Photovoltaics. , 2006, , 167-185.		0
617	New education opportunities and research activities at UNSW. Proceedings of SPIE, 2007, , .	0.8	0
618	Study on boron doped silicon quantum dots superlattices for all-silicon tandem solar cells. Optoelectronic and Microelectronic Materials and Devices (COMMAD), Conference on, 2008, , .	0.0	0
619	Structural characterization of solid phase crystallized Si _{0.5} Ge _{0.5} films for photovoltaic applications. , 2009, , .		0
620	Measuring strain changes during production of thin film crystalline silicon on glass photovoltaic modules. Journal of Materials Science: Materials in Electronics, 2010, 21, 1207-1212.	2.2	0
621	Raman study of stress effect in silicon rich carbide (SiCX) film by furnace and rapid thermal annealing for photovoltaic application. , 2010, , .		0
622	Heavily Boron-Doped Hydrogenated Polycrystalline Ge Thin Films Prepared by Cosputtering. Electrochemical and Solid-State Letters, 2010, 13, H354.	2.2	0
623	Limiting recombination mechanisms in thin film silicon on glass solar cells. , 2010, , .		0
624	Photovoltaic effect in Ge nanocrystals/c-silicon heterojunctions devices. , 2010, , .		0
625	A ultra-thin silicon nitride barrier layer implementation for silicon quantum dots in amorphous silicon carbide matrix in photovoltaic application. Energy Procedia, 2011, 10, 271-281.	1.8	0
626	Effects of high temperature incubation on solid phase crystallisation of silicon films and properties of polycrystalline silicon thin-film solar cells on glass. , 2011, , .		0
627	The effect of rear surface passivation layer thickness on high efficiency solar cells with planar and scattering metal reflectors. , 2012, , .		0
628	Measurement of internal optical reflection characteristics of solar cell back reflectors. , 2012, , .		0
629	Application of Ge quantum wells fabricated by laser annealing as energy selective contacts for hot-carrier solar cells. , 2012, , .		0
630	Material characteristics of crystalline Si thin-film solar cells on glass fabricated by diode laser crystallization. , 2013, , .		0

#	ARTICLE	IF	CITATIONS
631	Inorganic nanophotovoltaics. , 2013, , .		0
632	Growth of Highly (112) Oriented Cu ₂ ZnSnS ₄ Thin Film on Sapphire Substrate by Radio Frequency Magnetron Sputtering. Materials Research Society Symposia Proceedings, 2014, 1640, 1.	0.1	0
633	LIMITS TO PHOTOVOLTAIC ENERGY CONVERSION EFFICIENCY. Series on Photoconversion of Solar Energy, 2014, , 41-86.	0.2	0
634	Re-interpretation of Silver Optical Constants for Plasmonic Applications. , 2014, , .		0
635	Plasmonic rear reflectors for thin-film solar cells: design principles from electromagnetic modelling. , 2014, , .		0
636	Ultrafast charge generation and relaxation dynamics in methylammonium lead bromide perovskites. , 2015, , .		0
637	Nanostructured metallic rear reflectors for thin solar cells: balancing parasitic absorption in metal and large-angle scattering. , 2015, , .		0
638	Mechanical transfer of pre-annealed Ag nanowire network on ITO electrode for Cu ₂ ZnSnS ₄ solar cells. , 2016, , .		0
639	Dislocation density reduction of virtual Ge substrates by CW diode laser treatment. , 2016, , .		0
640	Towards 10% State-of-the-Art Pure Sulfide Cu ₂ ZnSnS ₄ Solar Cell by modifying the Interface Chemistry. , 2017, , .		0
641	Low temperature solution process for random high aspect ratio silver nanowire as promising transparent conductive layer. , 2017, , .		0
642	Germanium Template Assisted Integration of Gallium Arsenide Nanocrystals on Silicon: A Versatile Platform for Modern Optoelectronic Materials. Advanced Optical Materials, 2018, 6, 1701329.	7.3	0
643	ALD ZnSnO buffer layer for enhancing heterojunction interface quality of CZTS solar cells. , 2018, , .		0
644	Low-temperature epitaxial growth of Ge on Si, towards a cost-effective substrate for III-V solar cells. , 2018, , .		0
645	Boosting the efficiency of kesterite Cu ₂ ZnSnS ₄ solar cells by optimizing the heterojunction interface quality. , 2018, , .		0
646	Epitaxial Growth of Ge on Si by Magnetron Sputtering. , 2018, , .		0
647	Solution-processed ultrathin SnO ₂ passivation of Absorber/Buffer Heterointerface and Grain Boundaries for High Efficiency Kesterite Cu ₂ ZnSnS ₄ Solar Cells. , 2019, , .		0
648	High-efficient Cd-free CZTS solar cells achieved by nanoscale atomic layer deposited aluminium oxide. , 2019, , .		0

#	ARTICLE	IF	CITATIONS
649	Unveiling the Importance of Precursor Preparation for Highly Efficient and Stable Phenethylammonium-Based Perovskite Solar Cells. Solar Rrl, 2020, 4, 2070043.	5.8	0
650	Editorial for Stuart Wenham Special Issue. Progress in Photovoltaics: Research and Applications, 2021, 29, 1147-1148.	8.1	0
651	Solar Cell Efficiency Tables (Version 22). , 2018, , 63-71.		0